

*Report on DELP 1984 Cruises in the Middle
Okinawa Trough
Part V: Topography and Geology of the Central
Grabens and Their Vicinity*

Masaaki KIMURA¹, Ichiro KANEOKA², Yuzo KATO¹,
Satoshi YAMAMOTO¹, Ikuo KUSHIRO³, Hidekazu TOKUYAMA⁴,
Hajimu KINOSHITA⁵, Nobuhiro ISEZAKI⁶, Hideko MASAKI¹,
Atsushi OSHIDA¹, Seiya UYEDA² and Thomas W.C. HILDE⁷

- ¹) University of the Ryukyus
- ²) Earthquake Research Institute, University of Tokyo
- ³) Geological Institute, University of Tokyo
- ⁴) Ocean Research Institute, University of Tokyo
- ⁵) Department of Earth Sciences, Chiba University
- ⁶) Department of Earth Sciences, Kobe University
- ⁷) Department of Geophysics, Texas A and M University

(Received April 18, 1986)

Abstract

Detailed survey by means of PDR, single channel water-gun and air-gun, multi-channel air-gun, proton and three component magnetometers and dredger revealed five segments of central grabens which are located in the axis of the Okinawa Trough of the study area. These grabens are aligned en echelon. The "Iheya" Graben is the most pronounced. No positive evidence was found for the existence of transform faults connecting the en echelon grabens. A basaltic ridge and knolls were newly found in the central axis of these grabens. From these central knolls and the ridge pieces of olivine basalt were dredged. These are island arc type high alumina basalts with K-Ar ages younger than 1 Ma. Some rhyolite, dacite and a small quantity of dacitic andesite younger than 1 Ma (K-Ar and fission track ages) were also dredged in the vicinity, indicating bimodal volcanism. Thus, the petrologic evidence does not support the existence of an oceanic crust but it suggests an extensional stress field in the middle Okinawa Trough. Based upon the evidence, the middle Okinawa Trough is concluded to be in a rifting stage of an incipient spreading process in the continental margin.

1. Introduction

The Okinawa Trough (Fig. V-1) has been expected to be an area where the opening of a back-arc basin began in relatively recent years. It was the main purpose of the DELP-84 WAKASHIO Cruise to check this possibility in the middle Okinawa Trough area. This section is concerned with the topographic and seismic reflection surveys and dredge hauls conducted during the cruise. Some preliminary results of the survey and the study on rocks dredged will also be presented. Fig. V-2 shows the track lines of PDR, seismic reflection (single channel water-gun and air-gun) and magnetic survey, which are displayed in Figs. V-5 and V-15. Dredge locations are displayed in Fig. V-3. Fig. V-4 represents the submarine topography revised from that of KIMURA (1983) by adding the new data obtained during the DELP-84 WAKASHIO Cruise.

The Okinawa Trough is a big graben represented by the topographic depression behind the Ryukyu Arc. The width of the trough is 100-150 km and the length about 1200 km along the Ryukyu Arc. Thirteen en echelon grabens had been presented along the axis of the whole Okinawa Trough (Fig. V-1) which included some half-grabens. Those grabens had been regarded as central grabens (KIMURA, 1985).

The middle Okinawa Trough is one of most active places in the whole Okinawa Trough and the topographic features are very irregular. The water depth is between 1000-2000 m. Extensive young volcanic features are recognized in the trough-wide area by PDR and seismic reflection profiles. Plenty of Quaternary volcanic rocks were recovered from the features during the DELP-84 WAKASHIO Cruise. Sedimentary covers are very thin in the volcanic area. An earthquake swarm occurred in the area in 1980.

In the southern Okinawa Trough, the water depth reaches more than 2000 meters and the topographic features show a smooth sea floor except in the narrow central graben areas. Though young volcanic ridges had been recognized in the southern Okinawa Trough, they are limited to the very narrow central grabens offsetting Quaternary thick sedimentary layers (SIBUET *et al.*, 1986). The northern Okinawa Trough shows a shallower water depth of 500-1000 m and the sea floor is very smooth except for some knolls distributed in the margins of central grabens. Quaternary volcanoes have not been observed in this area.

2. Topography

In the study area, five topographic deeps limited to the axial part of the trough were recognized. These deeps were tentatively named the

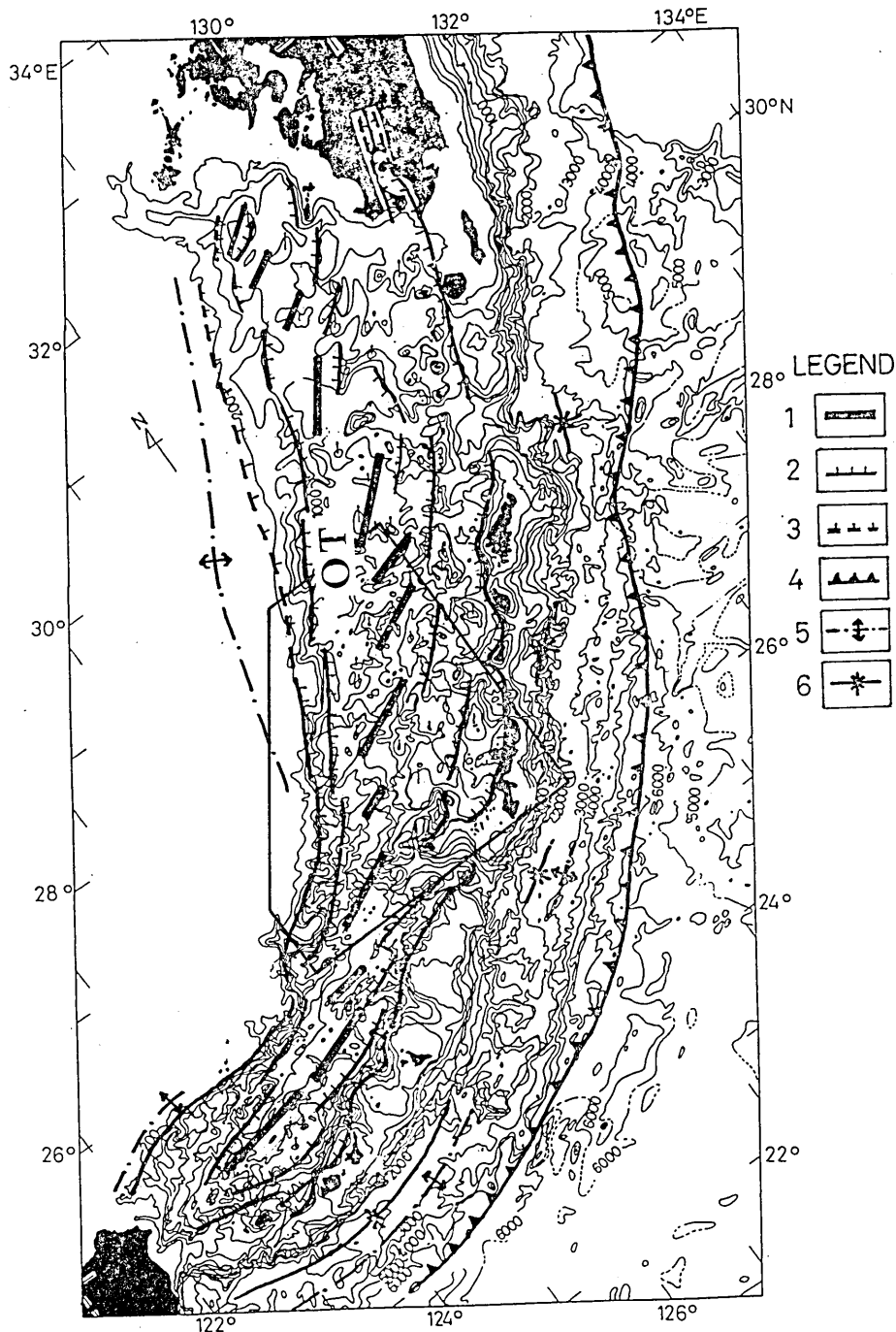


Fig. V-1. Morpho-tectonic map of the Ryukyu Arc region. Location of the study area is shown in the frame. The base map shows Quaternary rift system of the Okinawa Trough (KIMURA, 1985). Legend: 1, Central graben; 2, fault, hatching on the down thrown side; 3, buried fault; 4, trench; 5, anticline; 6, syncline. OT, Okinawa Trough.

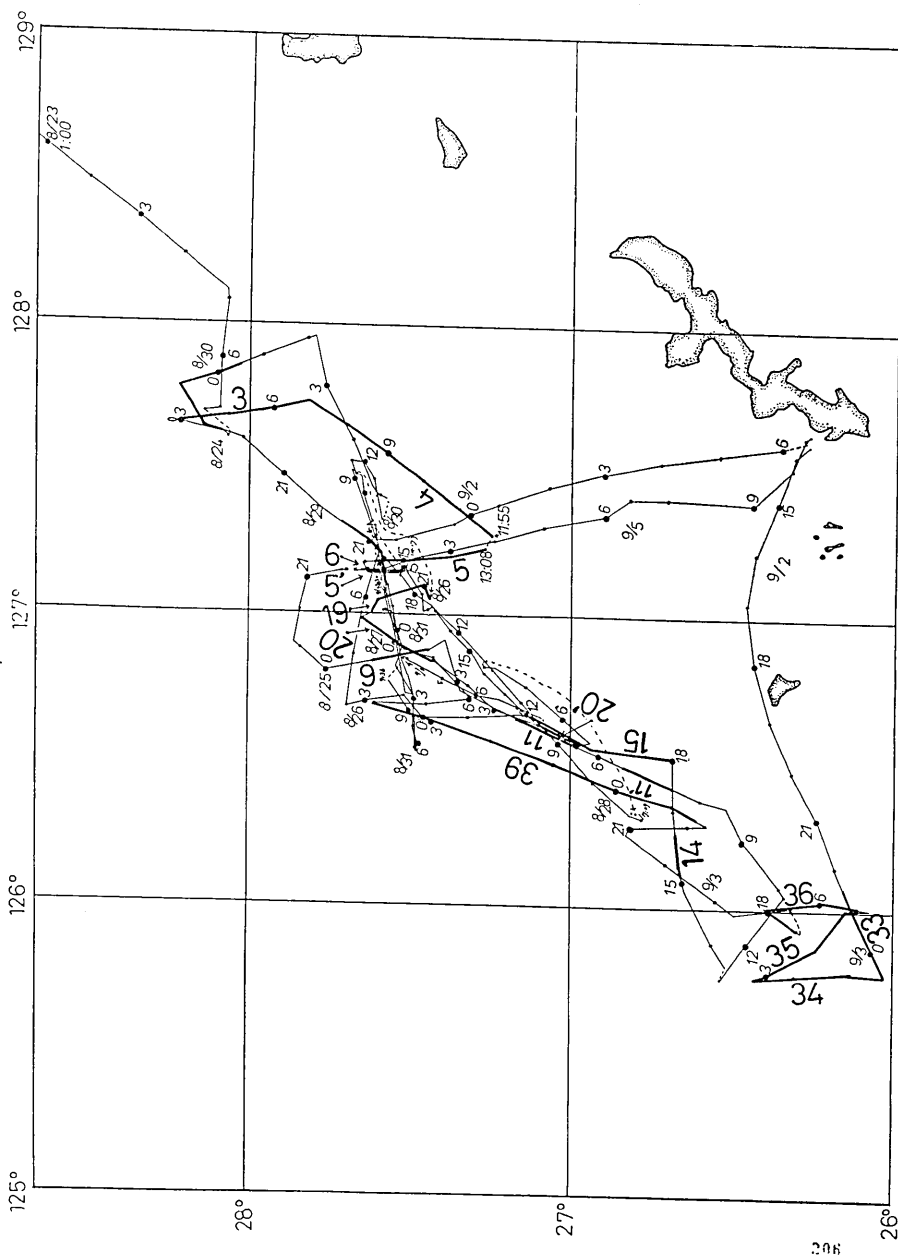


Fig. V-2. Location of profiles obtained during the DELP-84 WAKASHIO Cruise. Profiles are displayed in Figs. V-5 and V-15.

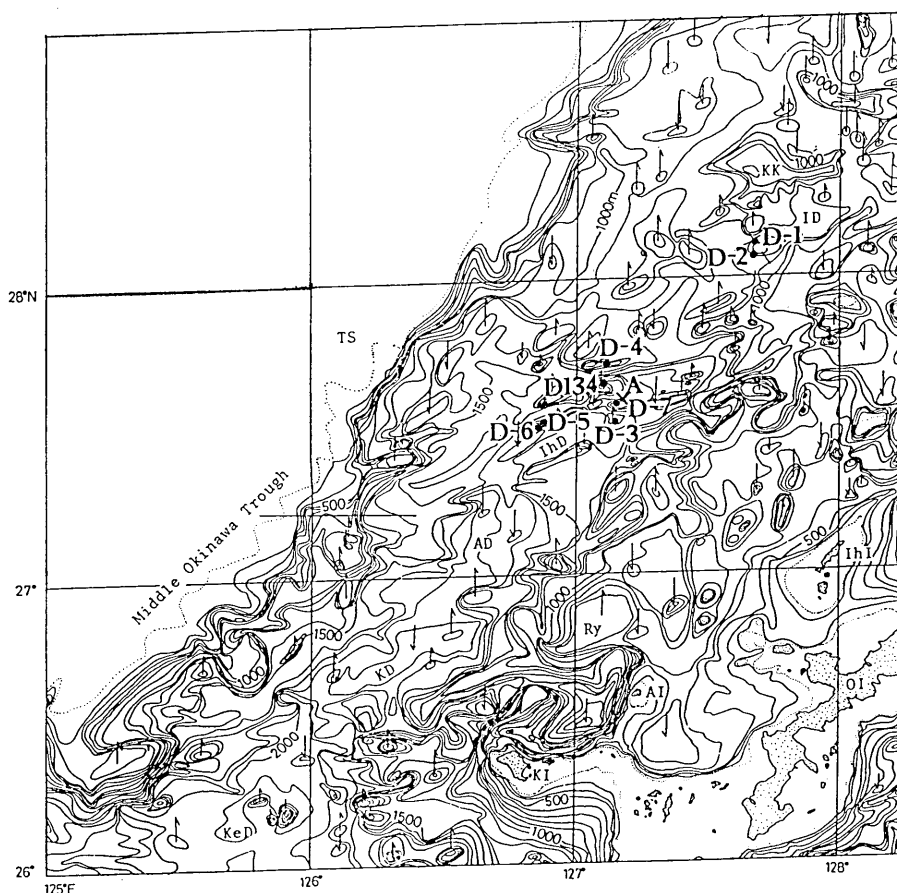


Fig. V-3. Sites for rock sampling carried out by the DELP-84 WAKASHIO Cruise (D-1—D-6), the "SHINKAI 2000" dives and a previous cruise of the Geological Survey of Japan. The sample SU 8491303 was taken at dive site A by the submersible "SHINKAI 2000". D134 rock had been dated by SHIBATA *et al.* (1984). KK, Karuishi Knoll; ID, Ito Deep; Ihd, Iheya Deep; AD, Aguni Deep; KD, Kume Deep; KeD, Kerama Deep; IhI, Iheya Islands; AI, Aguni Island; OI, Okinawa Islands; TS, Tsunghai Shelf.

Karuishi, Iheya, Aguni, Kume and Kerama Deeps from the north to the south (Fig. V-4). It has been newly found that there are knolls and a ridge in the axial part of the deeps. These were also recognized by the seabeam survey by the R/V Jean Charcot POP-1 Cruise (SIBUET *et al.*, 1986) in 1984 carried out just after the DELP-84 WAKASHIO Cruise. They are regarded as a central ridge or knolls of the Okinawa Trough. The prominent central ridge in the axial part of the western portion of the Iheya Deep (Figs. V-5 and V-6F) is tentatively named the "Iheya Ridge". The Iheya Ridge is 2-3 km wide and at least 20 km long, oriented

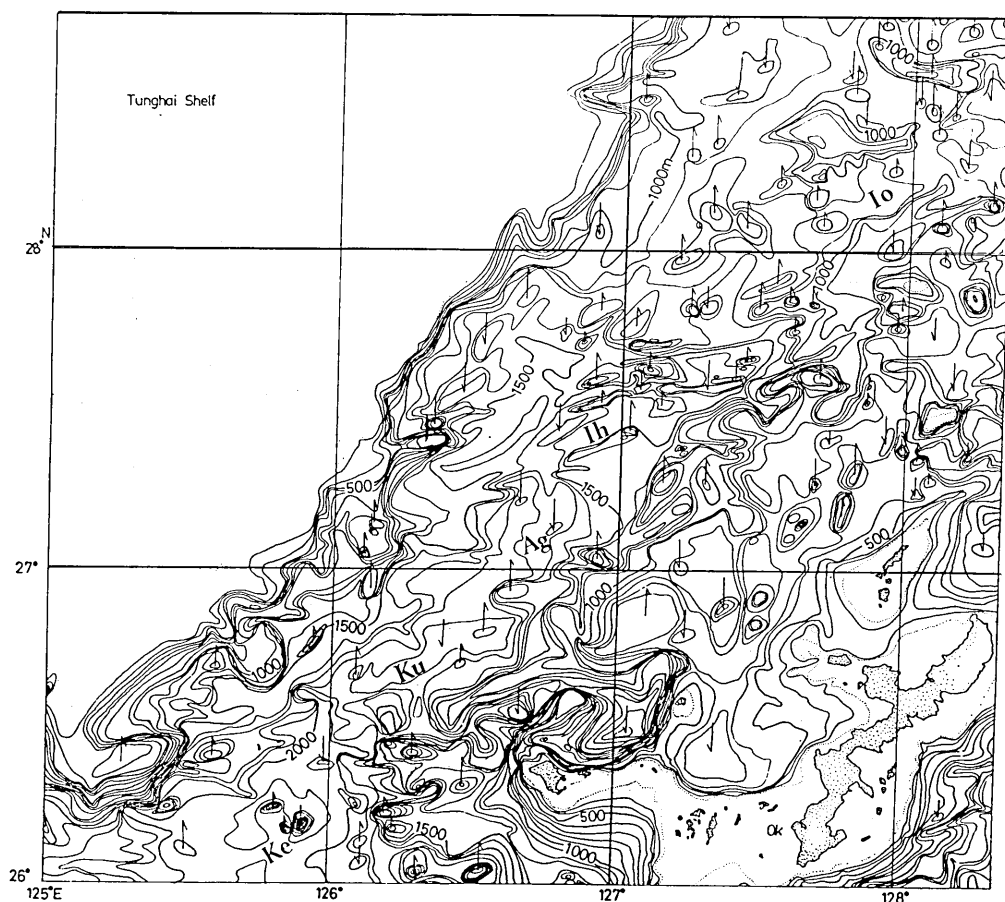


Fig. V-4. Submarine topographic map (100m contour interval) used as a base map of the present report. This map is revised from KIMURA (1983) by adding the new data from the DELP-84 WAKASHIO Cruise. Io, Io Deep; Ih, Iheya Deep; Ag, Aguni Deep; Ku, Kume Deep; Ke, Kerama Deep.

from the west to the east. The relative height of the Iheya Ridge is about 300m. Plenty of basalt samples were dredged from the ridge (D-5 and D-6 in Fig. V-3 and Table V-1). Central knolls were recognized in the other four deeps (Fig. V-3).

3. Petrochemistry of volcanic rocks

Lava and pumice were sampled during the DELP-84 WAKASHIO Cruise (Plates V-1, V-2, V-3, V-4, Tables V-1 and V-3) and during the dives of the submersible "SHINKAI 2000" (UYEDA *et al.*, 1985) (Tables V-2 and V-3).

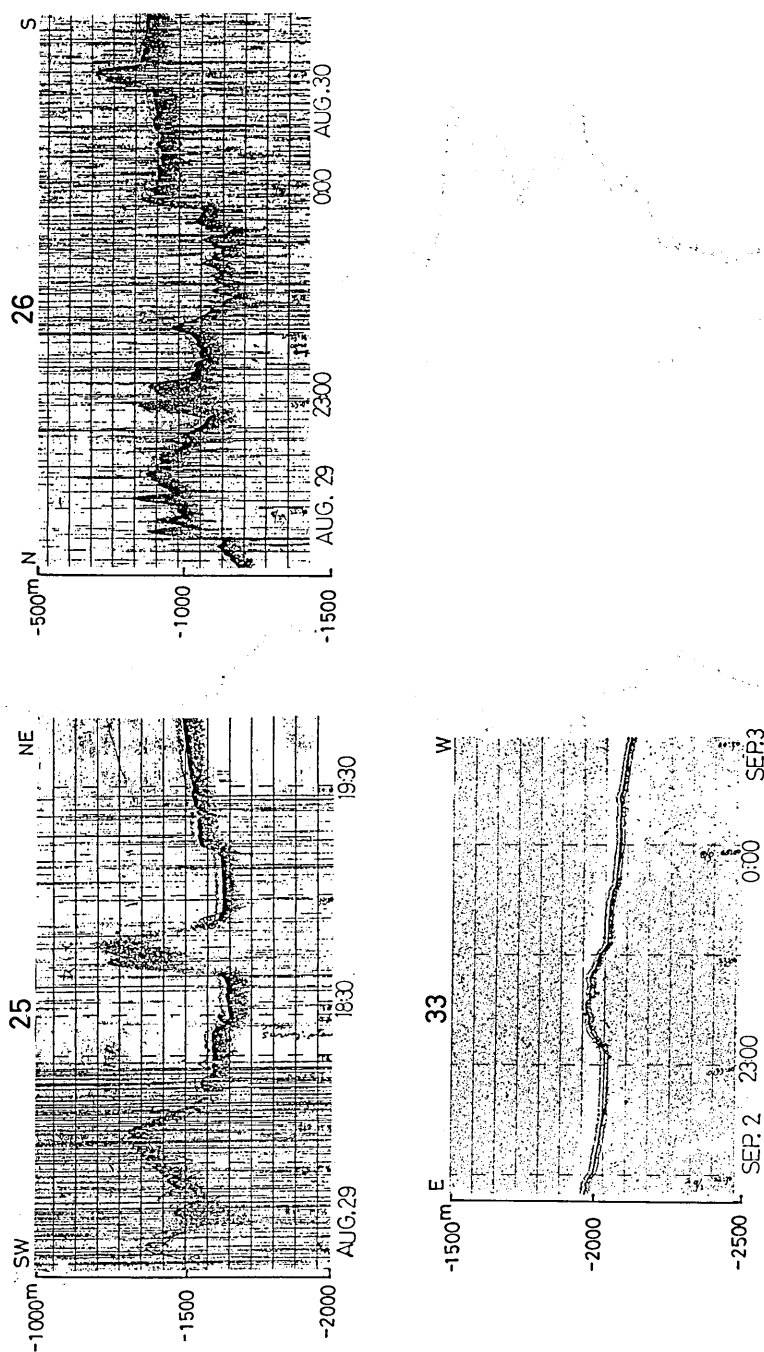


Fig. V-5. (A)

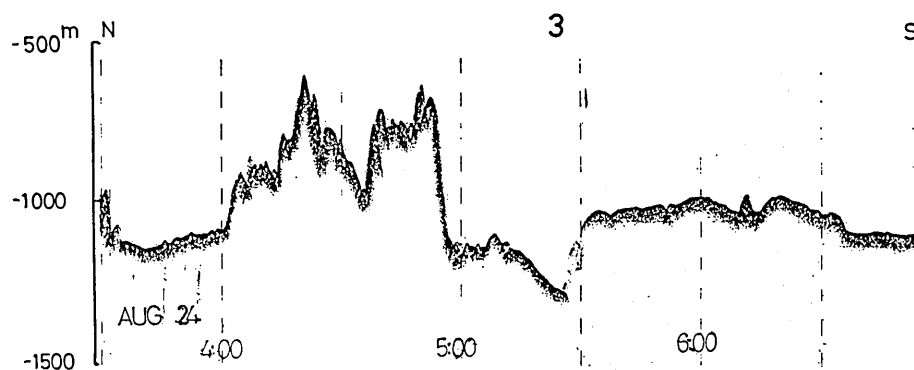


Fig. V-5. (B)

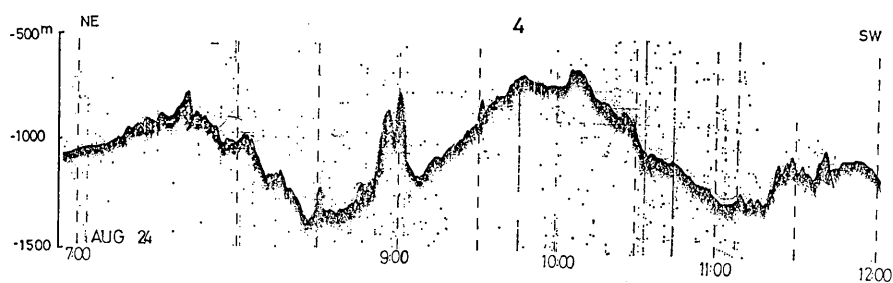


Fig. V-5. (C)

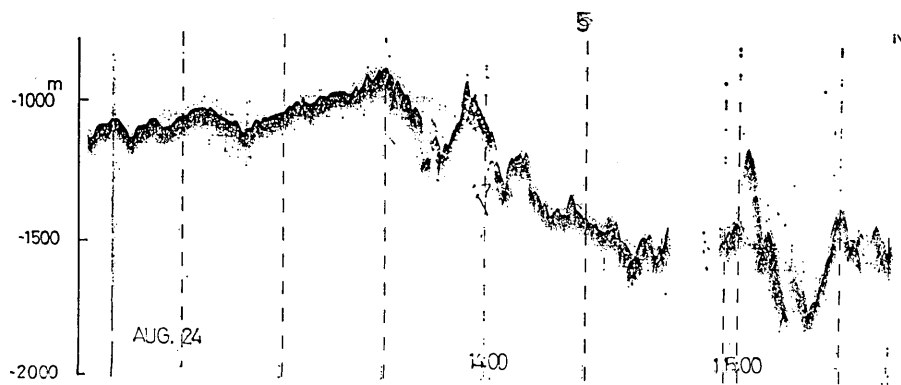


Fig. V-5. (D)

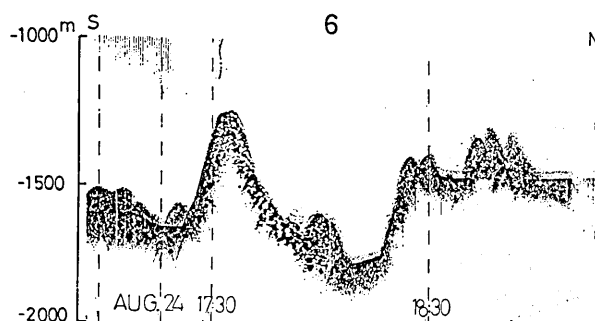


Fig. V-5. (E)

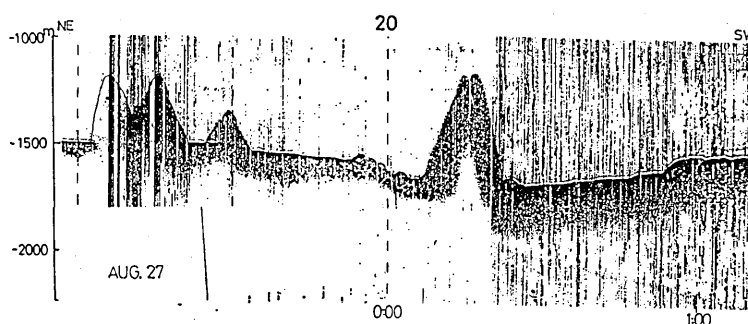


Fig. V-5. (F)

a) Lava

Under the microscope, all the rocks are more or less glassy suggesting that they were quenched by water. The chemical compositions are given in Table V-4. As the table shows, rocks are bimodal in composition, i. e., they are composed of basalt and dacite with a small amount of acidic andesite, lacking in intermediate to basic (53-63% in SiO_2 content) andesite.

Compositions of basalt are plotted on $\text{Al}_2\text{O}_3-(\text{Na}_2\text{O}+\text{K}_2\text{O})-\text{SiO}_2$ diagram (Fig. V-6A). The diagram demonstrates that all basalt samples belong to the high-alumina basalt series.

Dacite and acidic andesite are plotted in the field of hypersthene rock series in $\text{MgO}-\text{FeO}^*-(\text{Na}_2\text{O}+\text{K}_2\text{O})$ diagram (Fig. V-6B). These rocks contain hornblende phenocryst. These two pieces of evidence show that the acidic rocks belong to the calc-alkaline series.

The fact that all basalts belong to high-alumina basalt series and that the rocks are bimodal in composition indicates that this rock suite has the character of volcanics generated under an extensional tectonic environment (LIPMAN *et al.*, 1972; KONDA, 1973).

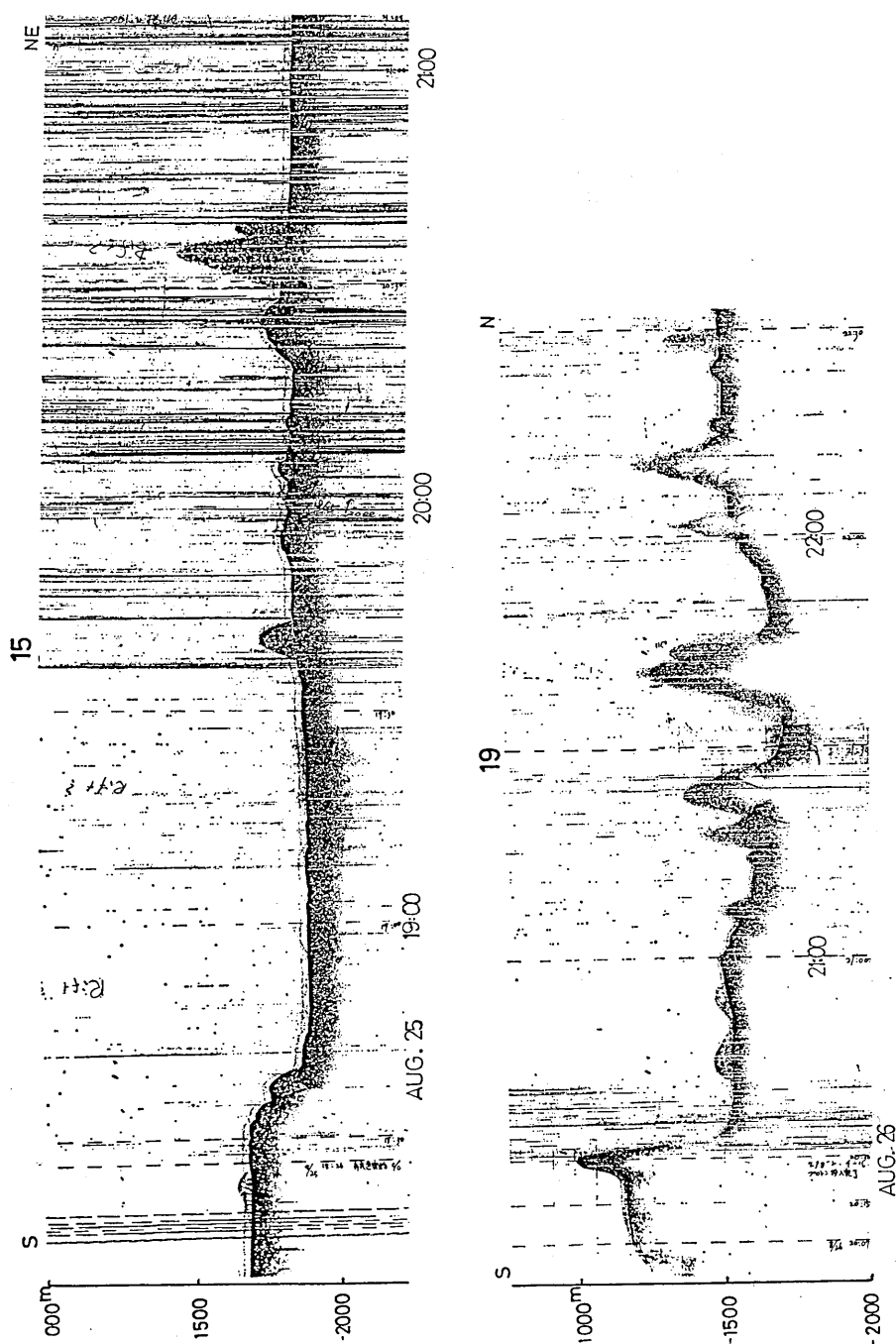


Fig. V-5. (G)

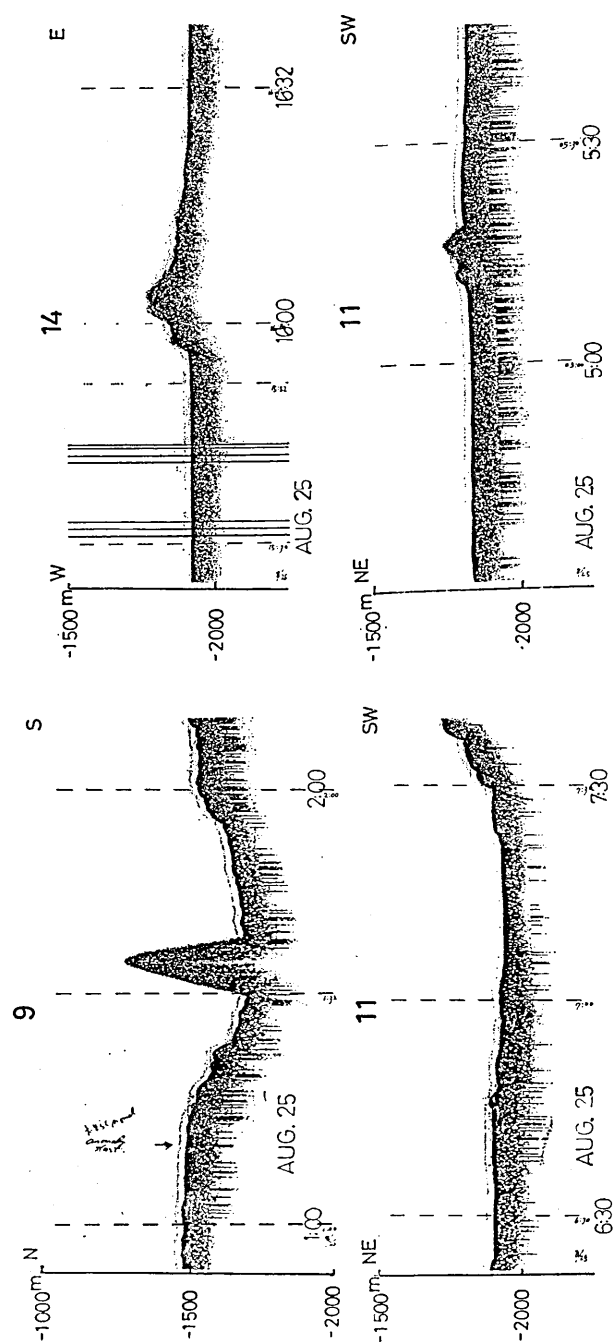


Fig. V-5. (H)

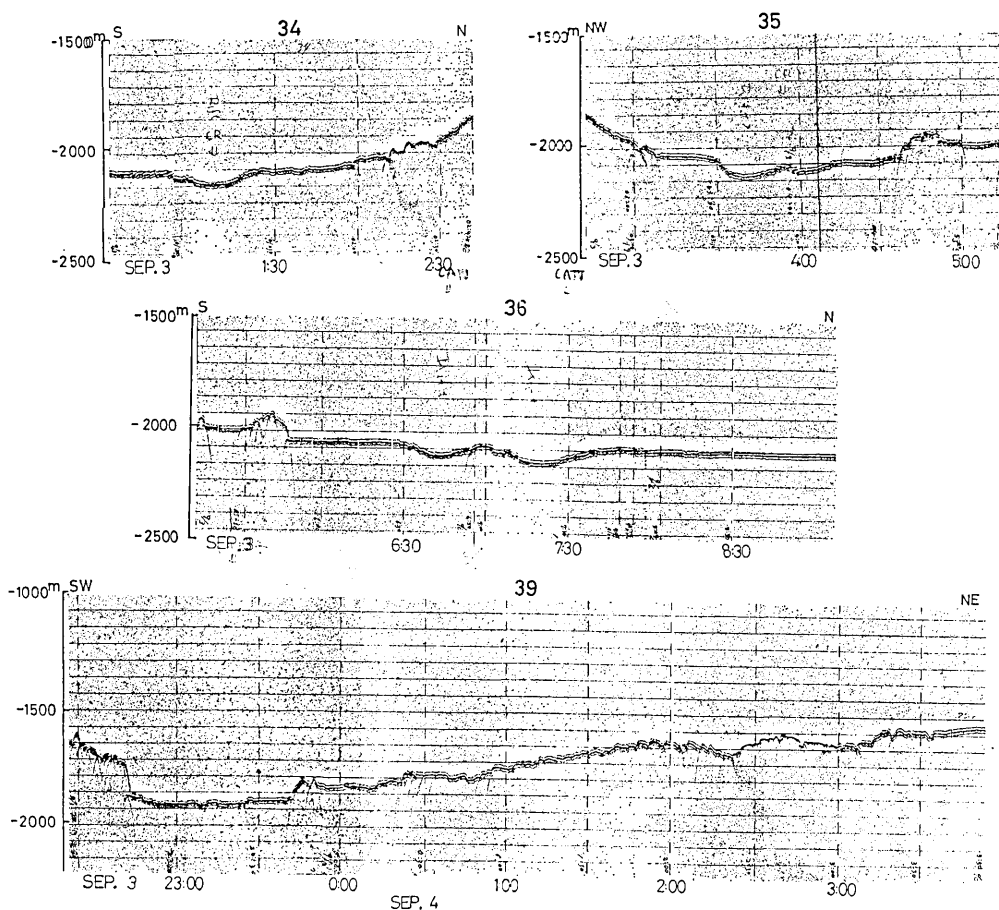


Fig. V-5. (I)

Fig. V-5. Submarine topographic PDR profiles. Locations are shown in Fig. V-2.

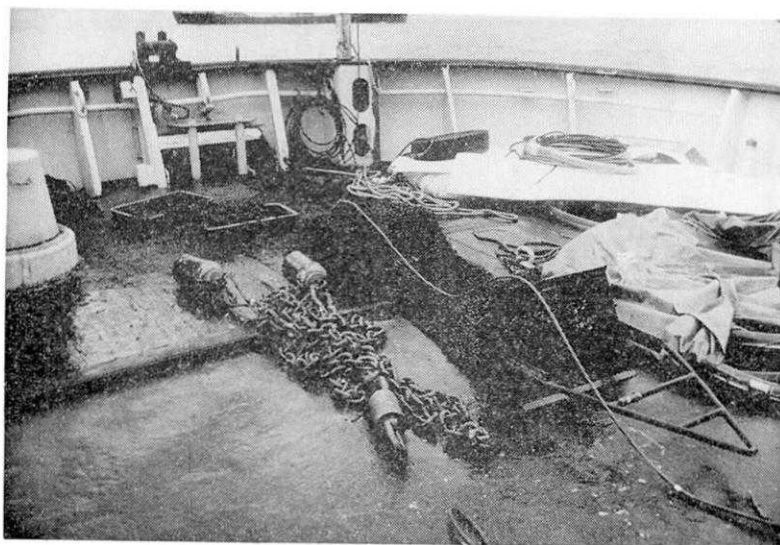
b) Pumice

The chemical compositions of pumice samples are given in Table V-5. In $\text{MgO-FeO}^*-(\text{Na}_2\text{O}+\text{K}_2\text{O})$ diagram (Fig. V-6B), they are divided into two groups. The first group shown by open-dot circles, (Nos. 3 and 4 in Table V-3-(2) and Table V-5), is plotted on the variation trend of lava, while the other group shown by open circles, is plotted near to $\text{FeO}^*-(\text{Na}_2\text{O}+\text{K}_2\text{O})$ join, apart from the variation curve. This fact suggests that pumice of the former group is comagmatic with acidic member of lava, i. e., dacite and acidic andesite.

Table V-1. Dredge stations (DELP-84 WAKASHIO Cruise).

Dredge station	Date	Time	Position		Depth (m)	Sampler	Area and topography	Samples
			Latitude (N)	Longitude (E)				
D-1	1984 August, 23	8:58	28°07.30'	127°40.50'	890	Chain-bag type dredge	Southern slope of the Karuishi knoll in the Central Graben.	Several pieces of glassy basalt blocks (Max. size 20×20×5 cm). Scoria (lapilli size). Pumice blocks (Max. size 17×15×10 cm). Small amount of pale bluish gray soft sediment. Total weight of rock samples; 70 kg.
		9:44	28°07.50'	127°40.40'	846			
D-2	August, 23	18:10	28°04.28'	127°40.15'	1160	ditto	Top of the central mound in the Central Graben.	Angular pumice blocks coated with dark reddish matter (15×15×15 cm in average). Large amount of soft sediment. Total weight of rock samples; 25 kg.
		18:31	28°04.54'	127°40.00'	1150			
D-3	August, 28	16:30	27°30.92'	127°09.08'	1578	ditto	Central mound (diving area of the SHINKAI 2000), slope.	Pumice blocks (Max. size 24×23×13 cm and abundant size 10×5×5 cm). Soft brown sediment. Total weight of rock samples; 25 kg.
		17:30	27°31.66'	127°08.17'	1200			
D-4	August, 29	0:50	27°40.07'	127°06.93'	1542	ditto	Southern slope of the knoll, north of the Central Rift.	No samples.
		1:16	27°43.75'	127°06.55'	1320			
D-5	August, 31	15:22	27°31.02'	126°52.12'	1458	ditto	Top of the Central Ridge in the Central Graben.	Two pieces of vesicular basalt (6×5×5 cm and 4×4×3 cm). Total weight; 1 kg.
		15:55	27°31.40'	126°52.51'	1530			
D-6	September, 1	2:20	27°30.28'	126°51.64'	1405	ditto	Southern slope of the Central Ridge in the Central Graben.	Glassy basalt blocks (Max. size 30×20×10 cm and abundant size 15×10×5 cm). Grayish brown mud. Total weight of rock samples; 70 kg.
		3:05	27°30.60'	126°51.53'	1437			
D-7	September, 4	14:37	27°34.96'	127°09.34'	1720	ditto	Southern slope of the knoll.	Soft sediment (1 kg) and pumice (less amount).
		16:33	27°09.34'	127°09.41'	1673			

(1)



(2)

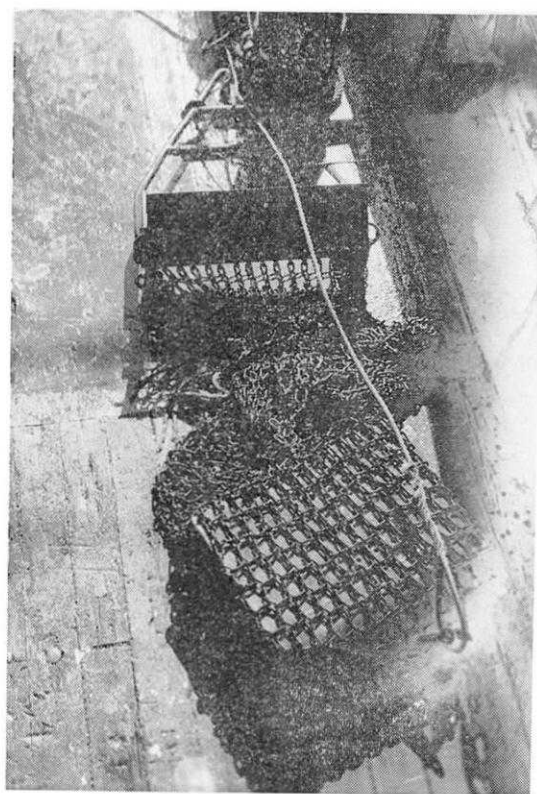


Plate V-1. Chain bag type dredger used for present study.
(1) Front view. (2) Back view.

(1)



(2)



(3)

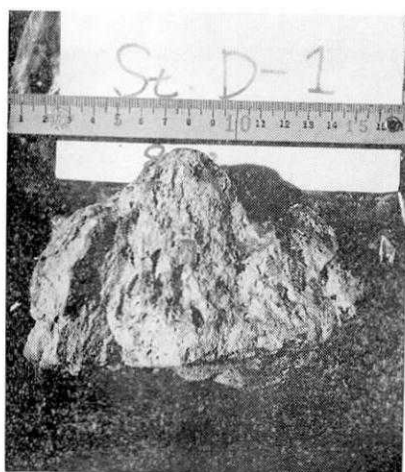


Plate V-2. Rock samples dredged (Dredge St. D-1).
(1) and (3), pumice blocks; (2), basalt blocks (left in the box) and
pumice blocks (right in the box).

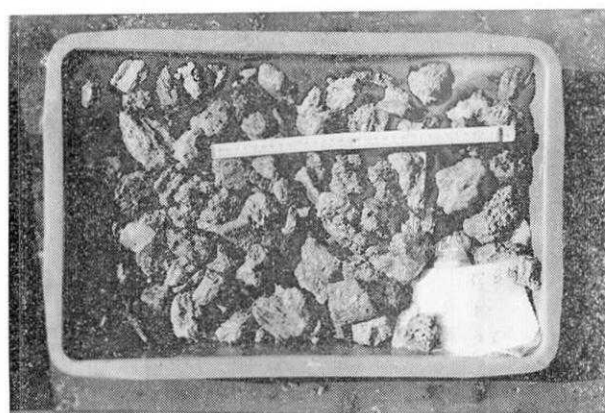
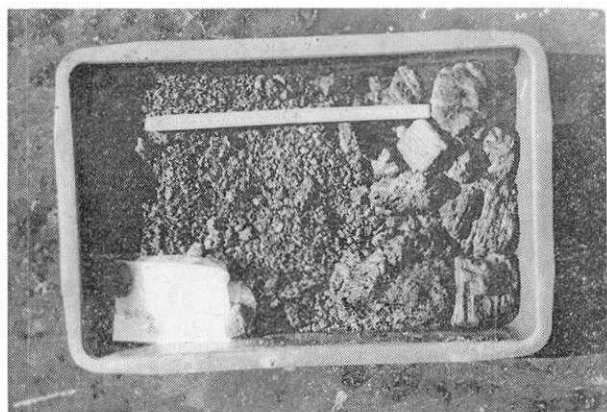


Plate V-3. Dredged pumice blocks (St. D-3).

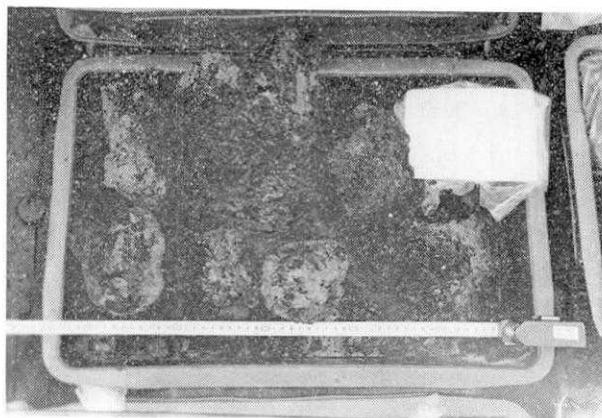


Plate V-4. Dredged basalt blocks (St. D-6).

Table V-2. Rock samples collected by the submersible "SHINKAI 2000" (UYEDA *et al.*, 1985).

Station	Latitude (N)	Longitude (E)	Water Depth	Volume	Number of Articles	Sample	Location
138-1	27°35.44'	127°08.93'	1750 ^m	Cm Cm Cm 20x20x15	1	Pumice	Rift valley floor
138-2	27°35.63'	127°08.78'	1750	20x20x15	1	Pumice	"
139-1	27°34.93'	127°08.31'	1630	22x20x15	1	Pumice	Slope of the knoll
139-2	27°34.87'	127°08.17'	1535	30x25x15	1	Dacite	Top of the knoll
140-1	27°34.79'	127°08.11'	1530	17x13x10	1	Pumice	Top of the knoll
140-2	27°34.80'	127°08.21'	1516	12x9x6	1	Dacite	"
140-3	27°34.77'	127°08.23'	1540	25x20x16 (10kg)	1	Andecite	"

Table V-3. Identified rock samples. Stations are represented in Tables V-1 and -2. Nos. 1, 4, 6, 9, 11 and 13 in Table V-3-(1) were identified by I. Kushiro and others by Y. KATO.

(1) Lava			
NO.	Station	Sample designation	Rock Name
1	D-1	D-1(B)	Olivine basalt
2		D-1YK	Olivine-bearing augite basalt (glassy)
3	D-6	D-6Ag1YK	Olivine-bearing augite basalt (glassy, Quenched part of No.5)
4		D-6(A)	Olivine-augite basalt
5		D-6AcRYK	Olivine-bearing augite basalt
6		D-6(B)	Olivine-bearing augite basalt
7		D-6BYK	Olivine augite basalt
8	140-3	13-3YK	Hornblende-bearing augite hypersthene andesite
9	140-3	SU8491303	Hornblende-bearing augite hypersthene andesite
10	140-2	13-2YK	Augite-bearing hypersthene hornblende dacite
11	D-1	D-1(A)	Dacite
12	139-2	12-2YK	Hypersthene hornblende dacite
13	D-3	D-3(D)	Dacite
(2) Pumice			
1	138-1	11-1YK	Pumice
2	138-2	11-2YK	"
3	139-1	12-1YK	"
4	140-1	13-1YK	"
5	D-1	D-1BPYK	"
6		D-1APYK	"
7	D-3	D-3PYK	"

4. K-Ar ages of some volcanic rocks recovered from the Middle Okinawa Trough

4.1. Samples

Dated samples include a hornblende-bearing augite hypersthene

Table V-4. Chemical Composition of lava samples. Nos. 1, 4, 6, 9 and 11 were analysed by H. HARAMURA, and others by Y. KATO. Nos. 2~12 are displayed in Table V-3-(1). Nos. 8, 10 and 12 are cited from KATO (in press). The Nos. are the same as in Table V-3.

No.	1	2	3	4	5	6	7	8	9	10	11	12
SiO ₂	49.96	50.35	50.41	50.57	50.82	52.06	52.51	63.17	63.71	68.48	70.67	71.57
TiO ₂	1.17	1.08	1.09	1.17	1.06	1.23	1.13	0.80	0.78	0.48	0.11	0.33
Al ₂ O ₃	17.66	17.32	16.18	16.79	16.47	16.19	16.00	16.28	15.89	14.57	12.49	13.56
Fe ₂ O ₃	1.87	1.94	1.30	1.80	1.58	2.01	2.13	1.83	2.27	1.24	0.61	0.79
FeO	8.01	7.78	8.27	7.90	7.88	7.66	7.40	3.06	2.98	1.93	1.41	1.54
MnO	0.24	0.25	0.18	0.27	0.17	0.26	0.21	0.12	0.13	0.09	0.08	0.06
MgO	5.83	6.03	6.39	5.69	6.24	5.41	5.79	1.51	1.51	0.83	0.33	0.51
CaO	11.61	11.14	11.39	11.36	11.18	10.20	10.09	4.41	4.50	2.64	1.33	1.88
Na ₂ O	2.61	2.52	2.86	2.71	2.84	3.18	3.02	4.75	4.73	4.65	5.80	4.51
K ₂ O	0.40	0.35	0.50	0.50	0.50	0.53	0.52	1.67	1.77	2.41	2.44	2.81
H ₂ O(+)	0.58	0.14	0.19	0.85	0.19	1.09	0.18	0.22	1.63	0.11	4.25	0.06
H ₂ O(-)	0.10	0.85	1.15	0.10	0.91	0.12	0.88	1.93	0.00	2.24	0.35	2.07
P ₂ O ₅	0.13	0.26	0.09	0.16	0.17	0.16	0.15	0.24	0.02	0.34	0.03	0.31
Total	100.17	100.01	100.00	99.87	100.01	100.10	100.01	99.99	99.92	100.01	99.90	100.00

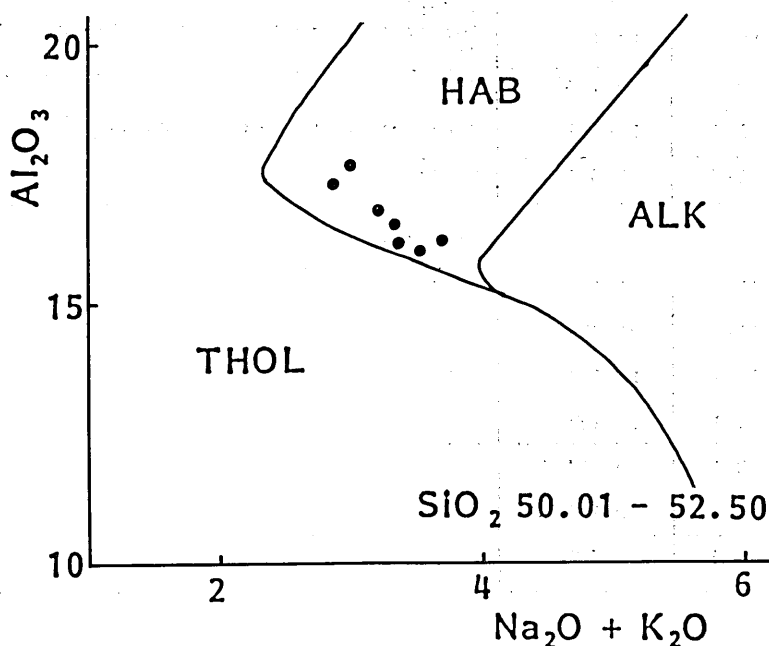


Fig. V-6 (A). Chemical compositions of dredged basalt by the DELP-84 WAKASHIO Cruise shown in Table V-4 (Nos. 1-7), plotted on $\text{Al}_2\text{O}_3 - (\text{Na}_2\text{O} + \text{K}_2\text{O}) - \text{SiO}_2$ diagram.

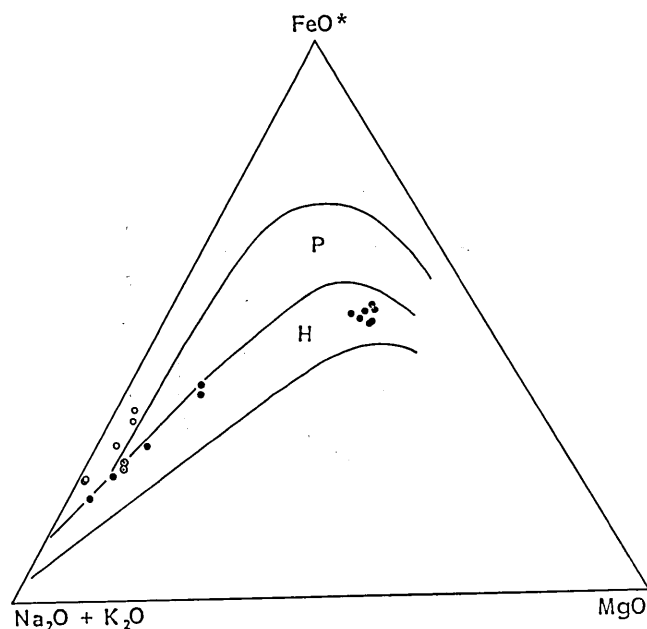


Fig. V-6 (B). $\text{MgO-FeO}^*-(\text{Na}_2\text{O}+\text{K}_2\text{O})$ diagram of lava and pumice collected by the DELP-84 WAKASHIO Cruise and the SHINKAI 2000. Fields of hypsithenic (H) and pigionitic (P) rock series of Izu-Hakone are based on KUNO (1954). Solid circle, lava; open-dot circle, pumice of the group plotted on variation trend of lava; open circle, pumice of the group plotted apart from the variation trend of lava. Pumice of the former group is inferred to be comagmatic with acidic members of lava, i. e., dacite and acidic andesite.

Table V-5. Chemical composition of pumice samples analysed by Y. Kato. Nos. 1~7 are displayed in Table V-3-(2). Nos. 1~4 are cited from KATO (in press).

	1	2	3	4	5	6	7
SiO_2	68.80	69.39	70.16	70.64	72.82	73.07	73.78
TiO_2	0.32	0.31	0.35	0.36	0.15	0.15	0.19
Al_2O_3	14.81	14.55	13.73	14.09	12.88	13.09	13.03
Fe_2O_3	0.96	0.75	0.86	0.79	0.57	0.57	0.63
FeO	3.25	3.13	1.72	1.73	1.64	1.60	1.93
MnO	0.15	0.20	0.13	0.06	0.09	0.08	0.10
MgO	0.34	0.40	0.62	0.64	0.19	0.14	0.28
CaO	2.36	2.27	2.12	2.14	1.31	1.28	2.09
Na_2O	5.55	5.52	4.61	4.51	4.85	4.76	4.78
K_2O	1.96	1.97	2.65	2.50	2.45	2.40	1.31
P_2O_5	0.06	0.06	0.06	0.06	0.01	0.01	0.01
$\text{H}_2\text{O}(+)$	1.42	1.26	2.65	2.36	2.87	2.66	1.78
$\text{H}_2\text{O}(-)$	0.00	0.18	0.34	0.11	0.17	0.19	0.10
Total	99.98	99.99	100.00	99.99	100.00	100.00	100.01

SU8491303

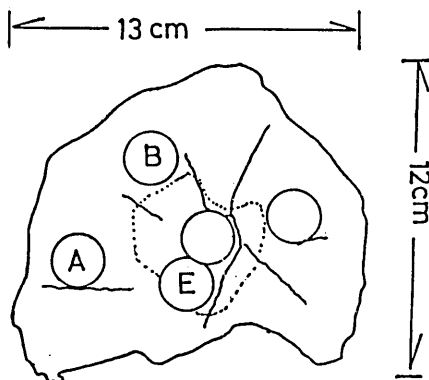


Fig. V-7. Schematic cross section of the sample SU 8491303.

andesite (SU 8491303) recovered in situ by "SHINKAI 2000" (UYEDA *et al.*, 1985) and olivine basalts (D-1 (B), D-6 (B)) and dacite (D-3 (D)) dredged during the DELP-84 WAKASHIO Cruise. Sampling sites are shown in Tables V-1, 2, 3 and Fig. V-2.

Under the microscope, these samples are relatively fresh, showing no apparent secondary products. The samples SU 8491303 contains no glassy part. However, the samples D-1 and D-6 are aphyric and contain glassy parts of more than 50~60%. The dacite sample D-3 is almost entirely glassy. Three cores, A, B and E, were drilled from the block SU 8491303 (Fig. V-7). Each portion was dated separately by the K-Ar method to check reliability. As shown in Fig. V-7, the samples SU 8491303B represent the outer portions, whereas sample SU 8491303E the inner one. If excess ^{40}Ar or some secondary processes such as alteration affected the K-Ar age of this sample, the obtained K-Ar ages would differ among different portions. For the DELP-84 WAKASHIO samples (D-1(B), D-3 (D), D-6(B)) only the innermost part was analysed.

4.2. Experimental

In the present study, the K content was determined by the XRF (X-ray fluorescence) method with an uncertainty of about 2%. Ar isotopes were analysed on a Reynolds type mass spectrometer (60°, 15 cm radius) and the amount of radiogenic ^{39}Ar was determined by the isotope dilution method with ^{38}Ar as tracer. The precision of Ar isotopic ratio measurement ranges from 0.5 to 2%, depending on the amounts of Ar isotopes. The uncertainty in a calculated K-Ar age includes those of the

Table V-6. K-Ar age of a volcanic rocks determined by I. KANEOKA (UYEDA *et al.* 1985). Sample name is represented in Table V-3-(1).

Sample	Rock Type	Weight (g)	K* (%)	$^{40}\text{Ar}_{\text{rad.}}$ ($\times 10^{-8}$ cm ³ STP/g)	$\frac{(^{40}\text{Ar})_{\text{air}}}{(^{40}\text{Ar})_{\text{tot.}}}$ (%)	K-Ar age ** (Ma)
SU8491303	Dacitic andesite					
(A)		1.794	1.45	1.25	97.2	0.22 \pm 0.06
(E)		2.442	1.42	1.34	98.2	0.24 \pm 0.18
(B)		1.208	1.42	(1.26)	94.7	(0.23)

* K content was determined by the XRF (X-ray fluorescence) method with the uncertainty of about 2%.

** K-Ar ages were calculated with the following values (STEIGER and JÄGER, 1977).
 $\lambda_e = 0.581 \times 10^{-10} \text{ yr}^{-1}$, $\lambda_\beta = 4.962 \times 10^{-10} \text{ yr}^{-1}$, $^{40}\text{K}/\text{K} = 1.167 \times 10^{-4}$ moles/mole.
 The uncertainty in the age represents one standard deviation. The amounts of $^{40}\text{Ar}_{\text{rad.}}$ for samples (A) and (E) were determined by the isotope dilution method with ^{38}Ar as a tracer, whereas that for sample (B) was determined by the peak height method.

Table V-7. K-Ar ages of volcanic rocks determined by I. KANEOKA. Sample name is shown in Table V-3.

Sample	Rock Type	Weight (g)	K* (%)	$^{40}\text{Ar}_{\text{rad.}}$ ($\times 10^{-8}$ cm ³ STP/g)	$\frac{(^{40}\text{Ar})_{\text{air}}}{(^{40}\text{Ar})_{\text{tot.}}}$ (%)	K-Ar age (Ma)
D-1(B)	Olivine basalt	1.637	0.347	0.39	99.5	0.29 \pm 0.78
D-3(D)	Dacite	0.365	2.03	~65	98.1	8.3 \pm 6.7
D-6(B)	Olivine augite basalt	2.317	0.470	0.773	95.8	0.42 \pm 0.19

* K content was determined by the XRF (X-ray fluorescence) method with the uncertainty of about 2%, except for the sample D-3 (D). As the K content for the sample D-3 (D), the value determined for a different block by the wet chemical method by H. Haramura was used.

statistical ones in Ar analysis together with those of the amount of the tracer and K measurements.

4.3. Results and discussion

Results are summarized in Tables V-6 and V-7, where the uncertainty in a K-Ar age represents 1σ (standard deviation).

For the sample SU 8591303, three portions show almost the same K-

Ar ages of 0.22~0.24 Ma. Among them, the amount of radiogenic ^{40}Ar for SU 8491303B was determined by the peak height method. Hence, the calculated age includes more uncertainty than the other two portions whose radiogenic ^{40}Ar was analysed by the isotope dilution method. Therefore, a weighted mean K-Ar age has been calculated from SU 8491303A and SU 8491303E, excluding SU 8491303B. The calculated age is 0.22 ± 0.08 Ma. Since this sample contains little glassy part and is relatively fresh, the K-Ar age would be close to the solidification age of this sample. Although the sample SU 8491303 was taken directly from a cliff facing the bottom of the Okinawa Trough by the submersible "SHINKAI 2000" it shows no chilled margin. Such a portion might have been removed already from the surface, which implies that the formation age of the cliff may not be very young. The obtained K-Ar age is compatible with such an interpretation.

On the other hand, the DELP-84 WAKASHIO samples show a large variation in the calculated K-Ar ages. The sample DELP-84 D-1 (B) indicates a K-Ar age almost indistinguishable from zero age if we consider its uncertainty. The sample DELP-84 D-6 (B) indicates a K-Ar age of 0.42 ± 0.19 Ma, which is apparently older than sample SU 8491303. Furthermore, the dacite (DELP-84 D-3 (D)) shows a much older K-Ar age of about 8 Ma, through the uncertainty in the calculated age is quite large. However all these rocks are quite glassy, as can be seen under a microscope. It is well known that quenched pillow contains quite large amount of excess ^{40}Ar (*e.g.*, DALRYMPLE and MOORE, 1968; DYMOND and HOGAN, 1973). The amount of excess ^{40}Ar can be as much as $(2\sim3) \times 10^{-6} \text{ cm}^3\text{STP/g}$, depending on the cooling condition. The accumulated data on recent pillow basalts suggest that such excess ^{40}Ar is observed in a sample which shows a glass content of more than 50~60%. Present dredged samples show glass contents in this range. Furthermore, as shown in Table V-7, the analysed dredged samples contain $(0.4\sim65) \times 10^{-8} \text{ cm}^3\text{STP/g}$ of non-atmospheric ^{40}Ar . Hence we cannot preclude the possibility that most radiogenic ^{40}Ar observed in analysed DELP-84 samples might represent excess ^{40}Ar . Under a microscope, these samples are fresh and the possibility of Ar loss due to sample alteration is quite small. Hence, the apparent K-Ar ages of DELP-84 samples obtained in this study would show only the maximum formation ages.

In Fig. V-8, the present K-Ar age data are plotted together with a reported K-Ar age for a rhyolite (D134 in Fig. V-2, SHIBATA *et al.*, 1984) on a geological map of the Iheya Deep. As far as these data are concerned, it is possible that basaltic rocks erupted very recently, but felsic intermediate volcanic rocks might have been formed earlier. Hence the high heat flow observed in this area (Part IV of this report) might be

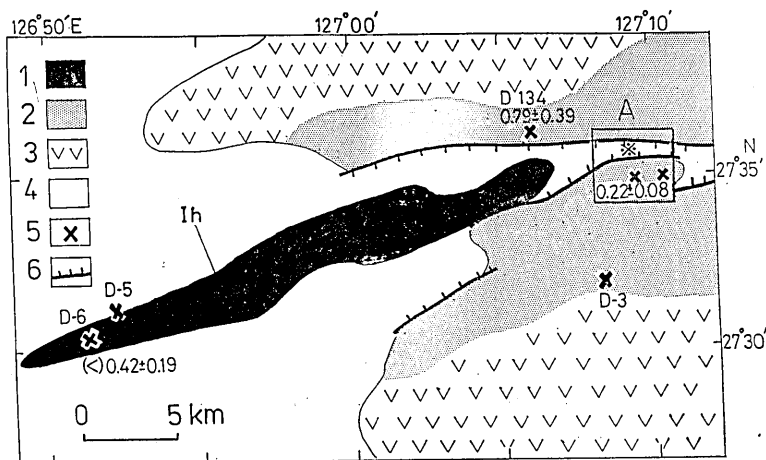


Fig. V-8. Submarine geologic map of the eastern Iheya Deep and the distribution of rocks dated by the K-Ar method. 1, Basalt; 2, Acidic volcanic rock; 3, Unidentified volcanic rock; 4, Sediment; 5, Sampling site; 6, Fault, teeth on the down thrown side. Ih is the Iheya Ridge; A is the dive site by the SHINKAI 2000. Asterisk (*) shows the location of the highest heat flow of over 1,600 mW/m² (YAMANO *et al.*, 1986).

related to the volcanic activity of such basaltic rocks.

5. Geochemical characterization of bottom sediments in the Okinawa Trough and its adjacent floors of the East China Sea.

5.1. Sedimentological and stratigraphic features of bottom sediments

The surface distribution of bottom sediments in the shelf areas of the East China Sea was studied extensively by NIINO and EMERY (1969) and the general patterns of distribution are well understood. However, the bottom sediments in the deeper Okinawa Trough have been sampled only sporadically and the type of sediment is poorly known. This section is intended to characterize the bottom sediments which were dredged from the Okinawa Trough during the DELP-85 WAKASHIO Cruise and to compare them with the bottom sediments in other parts of the East China Sea. The bottom sediments had also been dredged and cored from the continental shelves and slopes and the floors adjacent to the Okinawa Islands by several educational cruises (RN Cruises) of the University of the Ryukyus on R/V NAGASAKI MARU and the KT-84-14 (R/V TANSEI MARU) Cruise. The descriptions of RN-sediments were made elsewhere by YAMAMOTO *et al.* (1984).

Locations of dredged and cored samples which are investigated in this study are shown in the bathymetric map of Fig. V-9, and the sedi-

mentological characteristics of the analyzed samples are summarized in Table V-8. The analyzed samples include three piston cores (RN-80 PC-3, RN-82 PC-2 core catcher, and KT-84-14 P-1) and three cores from Smith-McIntyre sampling (RN-84 SM-1 through SM-3) in addition to dredged samples from 9 sites.

According to the distribution patterns of bottom sediments summarized by NIINO and EMERY (1969), the continental shelf area is distributed with sand except for the coastal areas and the tongue-like areas of the central portion where deltaic muds are distributed, but the sediments become finer than sand in the area off the continental slopes towards the Ryukyu Island Arc. Such a tendency is well recognized in Fig. V-10 which shows a generalized distribution pattern based on the present study. However, shallow floors off several islands of the Ryukyu Arc were not studied by NIINO and EMERY (1969). The recent studies by UJIE *et al.* (1983) and YAMAMOTO and UJIE (1983) have shown that biogenous calcareous sand is distributed in these areas. The color of offshore muddy sediments also shows some generalized patterns as indicated in Fig. V-10. Although the offshore muds may be grayish in most parts of the continental slope, some parts of the surface floors of the Okinawa Trough and trench slopes are covered by reddish brown mud. Such a brown mud appears to cover the surface floors of the basaltic exposures and their adjacent areas (YAMAMOTO and OOMORI, 1984). It may be an oxidized product by biological and other reactions (MASUZAWA, 1983).

In this study, the surface reddish brown muds were carefully examined to characterize their distribution patterns and stratigraphy. The stratigraphic features of the cored samples are shown in Figs. V-11 and V-12. No cover of brown mud is recognized for the grayish sand and mud in the continental shelf and slope areas, but, as mentioned above, covers of brown mud can be recognized in some parts of the Okinawa Trough and the trench slope area. In the KT-84-14 P-1 core, about a 35 cm thick layer of brown mud is observed together with bioturbation and burrows in the layer. The contact with the grayish silty clay is also bioturbated (Fig. V-12).

5.2. Geochemical analyses and characterization

Heavy metals and other metallic elements were leached and analyzed for different types of sediments. Table V-8 indicates the results of analyses with some sedimentological characteristics. The sediment samples were dried and powdered. 200 mg of the powdered samples was leached overnight with 10 ml of 10% (2.86N) HCl. Carbonates and other materials soluble by 10% HCl were dissolved completely with occasional shakings.

Table V-8. Results of chemical analyses by S. Yamamoto. Sample locations are shown in Table V-1 and Fig. V-9.

Sample designation	Geographic regions ²	Ca (%)	Sr (ppm)	Na (%)	K (ppm)	Fe (%)	Mg (%)	Mn (ppm)	Cu (ppm)	Ni (ppm)	Zn (ppm)	Cr (ppm)	Co (ppm)	Pb (ppm)	Sol. ¹ (%)	Sedimentological characteristics
DELP84 D-2	OT	8.81	262	0.518	2160	2.32	1.02	648	13.3	17.0	10.2	9.1	7.7	10.4	38.2	Grayish silty foram sand
DELP84 D-3a	OT	7.73	258	1.42	1800	2.08	0.916	3970	27.4	21.0	12.6	9.1	7.7	16.7	38.5	Dark brownish silty clay with pumice
DELP84 D-3b	OT	7.57	246	1.15	1700	1.96	0.864	3620	26.2	24.0	12.0	6.8	7.7	18.7	37.0	Dark brownish silty clay
DELP84 D-6	OT	9.99	297	1.11	1360	2.08	0.933	3360	27.4	23.0	12.4	6.8	9.6	25.0	43.1	Dark brownish silty (silty & foram sand)
DELP84 D-7a	OT	5.46	210	1.37	2410	3.26	1.05	901	21.7	24.0	48.6	9.1	9.6	20.8	33.1	Grayish silty clay
DELP84 D-7b	OT	4.74	205	1.81	2130	2.50	1.07	9750	42.1	25.0	85.6	9.1	11.5	43.8	32.8	Dark brownish clay
RN-81 D-2	CSB	9.81	271	0.769	4250	3.37	0.926	245	5.0	14.4	9.5	9.1	7.7	6.2	43.0	Dark grayish medium sand
RN-81 D-4A	OK	4.75	296	0.131	137	0.666	0.449	116	1.7	4.8	2.5	4.5	3.8	2.1	24.4	Sand with quartz, chert etc. (near the Kouri Isl.)
RN-82 PC-2 ^{cc}	OK	15.0	1070	0.769	1560	0.916	1.14	156	8.3	14.4	9.6	9.1	7.4	8.3	69.8	Grayish calcareous mud
RN-82 D-1	CSB	6.37	192	0.621	893	1.17	0.767	222	4.2	9.6	7.0	4.5	6.5	4.2	40.7	Dark grayish medium sand
RN-82 D-5	OK	16.7	1950	1.07	891	0.749	0.738	637	10.5	16.0	5.0	6.8	9.3	10.4	76.0	Grayish calcareous muddy sand (same above)
RN-82 D-6	OK	9.19	254	0.715	1030	1.17	0.732	163	9.7	11.0	7.5	6.8	5.6	4.2	38.5	Grayish sand (same above)
RN-84 SM-1 0-1 cm	CS	4.63	142	0.301	1350	1.38	0.652	336	3.2	9.0	8.9	4.5	4.6	6.2	28.8	(same above)
RN-84 SM-1 14-15 cm	CS	3.93	116	0.385	1220	1.12	0.472	173	2.4	8.0	7.4	4.5	5.6	4.2	25.5	(same above)
RN-84 SM-2 0-1 cm	CS	3.05	85.2	0.635	1690	1.63	0.802	491	4.0	12.0	8.0	6.8	4.6	4.2	24.1	(same above)
RN-84 SM-2 14-15 cm	CS	3.27	92.1	0.397	1560	1.56	0.767	276	4.2	10.6	8.5	6.8	5.6	4.2	21.5	(same above)
RN-84 SM-3 0-1 cm	CS	3.12	64.0	0.365	1830	1.69	0.820	345	4.2	11.5	10.6	6.8	5.6	6.2	21.4	(same above)
RN-84 SM-3 10-11 cm	CS	2.91	64.0	0.354	1940	1.75	0.882	310	4.2	11.5	8.9	4.5	6.5	4.2	34.5	Grayish mud (same above)
RN-84 SM-3 50-55 cm	CSL	5.81	216	1.25	2280	1.71	0.943	232	8.3	15.4	16.5	9.1	7.4	6.2	39.0	(same above)
RN-80 PC-3 120-125 cm	CSL	7.11	241	1.74	2320	2.11	0.987	233	7.5	13.5	10.3	9.1	7.4	4.2	24.2	(same above)
RN-80 PC-3 370-375 cm	CSL	1.47	29.1	1.53	3870	2.11	1.08	293	10.0	15.4	14.2	12.5	7.4	4.2	61.0	Brownish calcareous mud (same above)
KT-84-14 P-1 1-2 cm	TSL	13.1	559	0.988	1050	1.25	0.564	1010	36.4	19.2	10.6	7.5	10.7	8.3	53.7	(same above)
KT-84-14 P-1 17-18 cm	TSL	11.7	496	0.847	1160	1.25	0.705	1220	30.8	21.2	12.0	10.0	10.7	8.0	47.9	Grayish calcareous mud (same above)
KT-84-14 P-1 53-54 cm	TSL	11.5	394	1.06	2280	1.84	0.926	221	21.7	19.2	10.7	10.0	8.0	8.3	49.6	(same above)
KT-84-14 P-1 163-164 cm	TSL	12.0	403	1.06	2230	1.58	0.864	371	14.2	17.3	11.5	10.0	8.0	8.3	47.6	(same above & ash?)
KT-84-14 P-1 233-234 cm	TSL	12.1	428	0.957	1780	1.12	0.546	388	15.8	13.5	6.3	7.5	7.1	8.3	47.6	(same above)
KT-84-14 P-1 254-255 cm	TSL	10.5	453	1.04	2060	1.64	0.723	440	28.9	15.4	8.4	7.5	9.8	8.3	51.8	(same above)
KT-84-14 P-1 383-384 cm	TSL	9.84	314	0.899	2340	1.84	0.970	658	18.3	19.2	10.1	10.0	8.9	8.3	41.2	(same above)

¹ Weight percent of soluble fraction by 10% (2.8N) HCl² Abbreviations of geographic names:

CS---Continental shelf CSB---Continental shelf break

OK---off the Okinawa Islands TSL---Trench slope

CSL---Continental slope

OT---Okinawa Trough

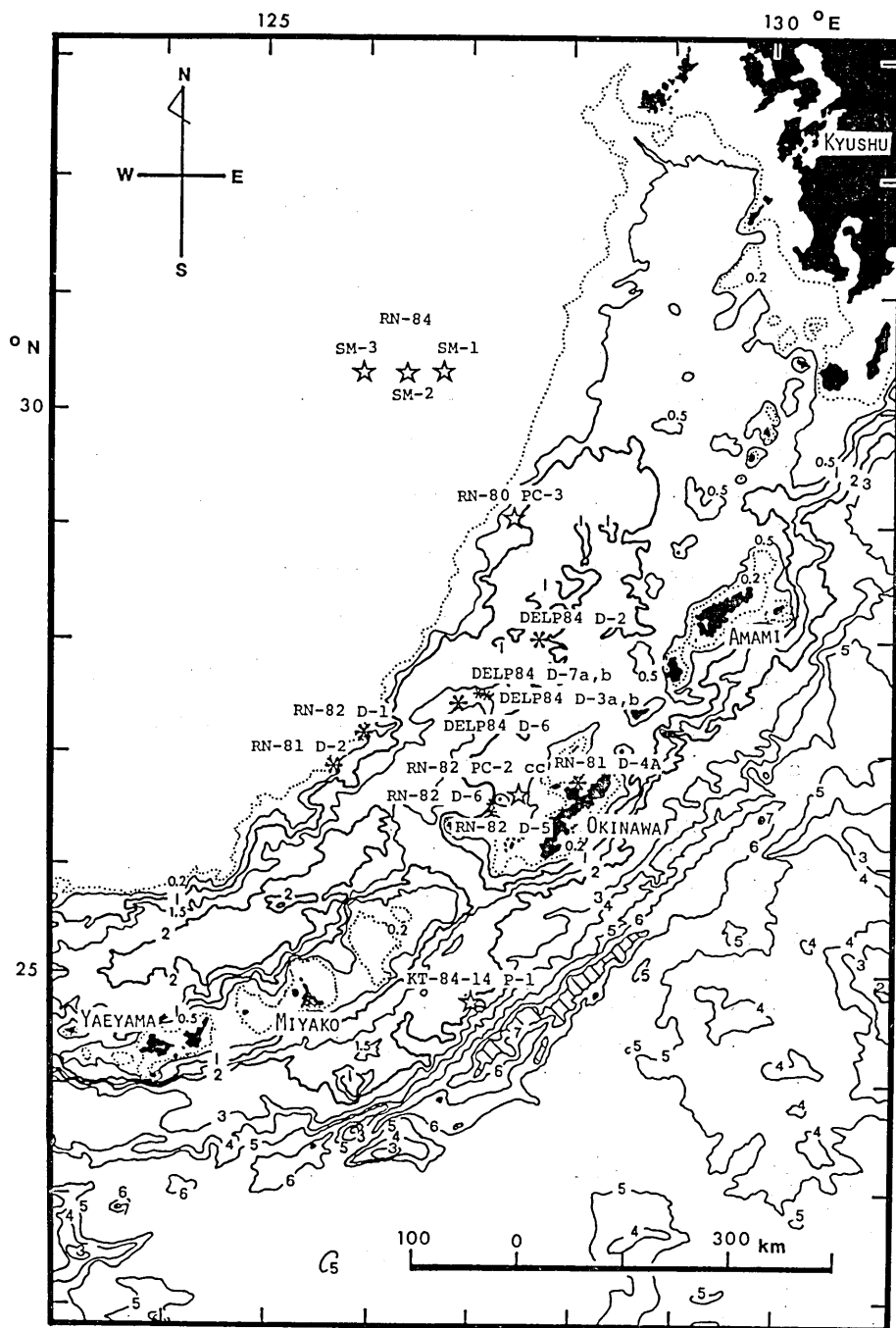


Fig. V-9. Site locations of sediment samples shown in Table V-8. Bathymetric contours are shown in km. Sites of dredging stations (asterisk, *) and coring stations (star, ☆) are indicated together with labels of site designations.

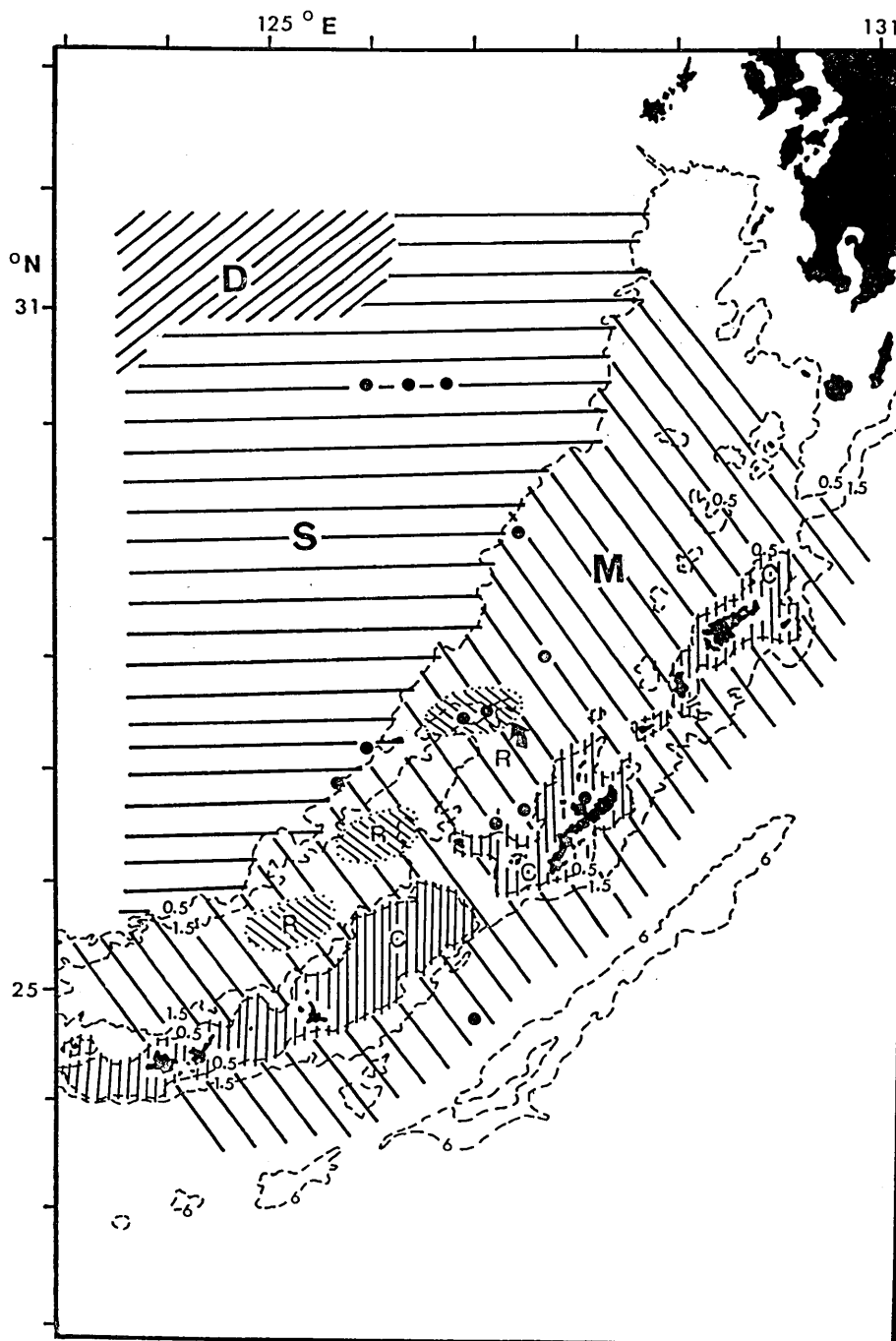


Fig. V-10. Generalized map of distribution patterns of bottom sediments. Bathymetric contours are shown in km. Patterns are labelled as D; Deltaic mud—sandy mud, S; Arkosic sand—muddy sand, M; Grayish mud (calcareous), locally its surface may be oxidized to brown mud, R; Reddish brown mud (igneous origin?), C; Calcareous sand—muddy calcareous sand. Sampling positions of the present study are indicated by dots (·).

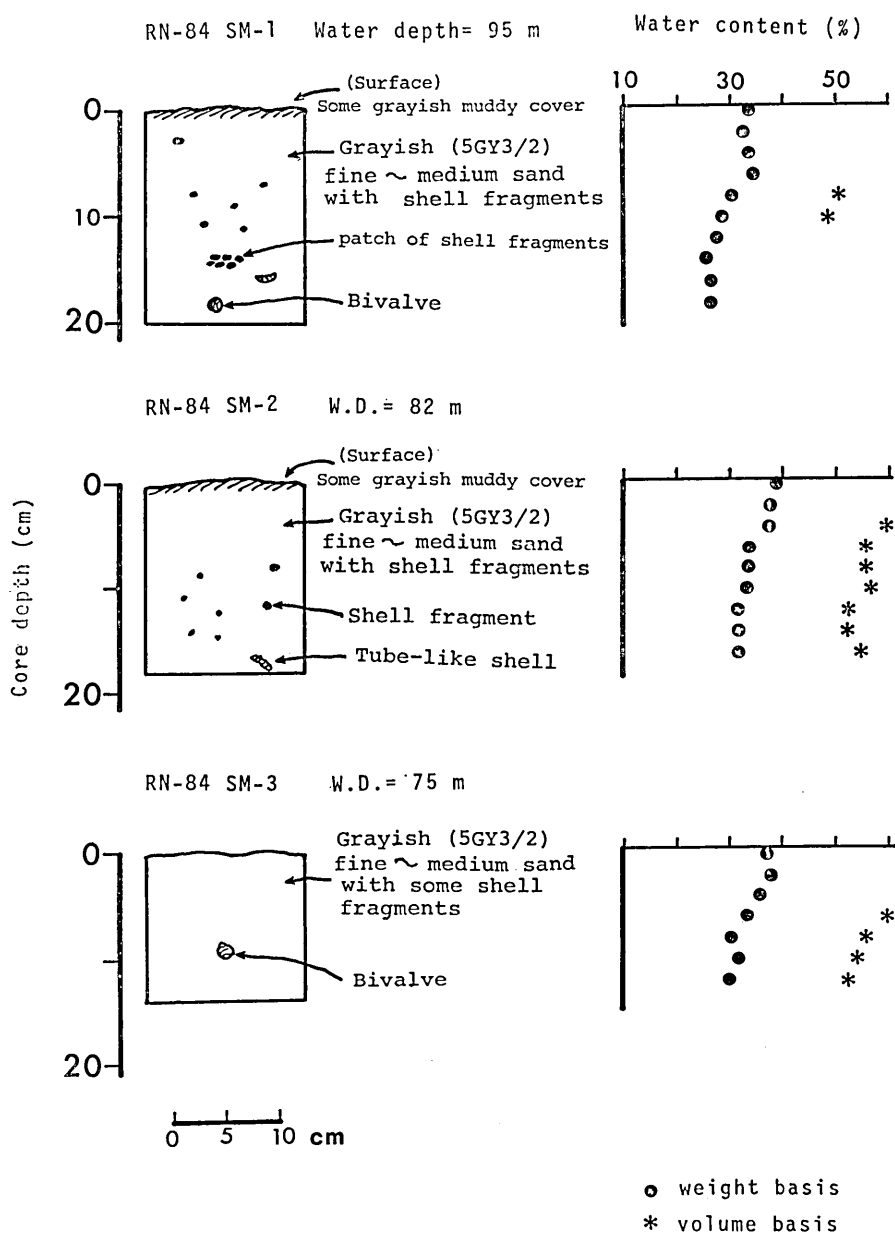


Fig. V-11. Lithologic descriptions of Smith-McIntyre cores from the continental shelf. Water contents were measured by determining the amount of sea-water loss on drying.

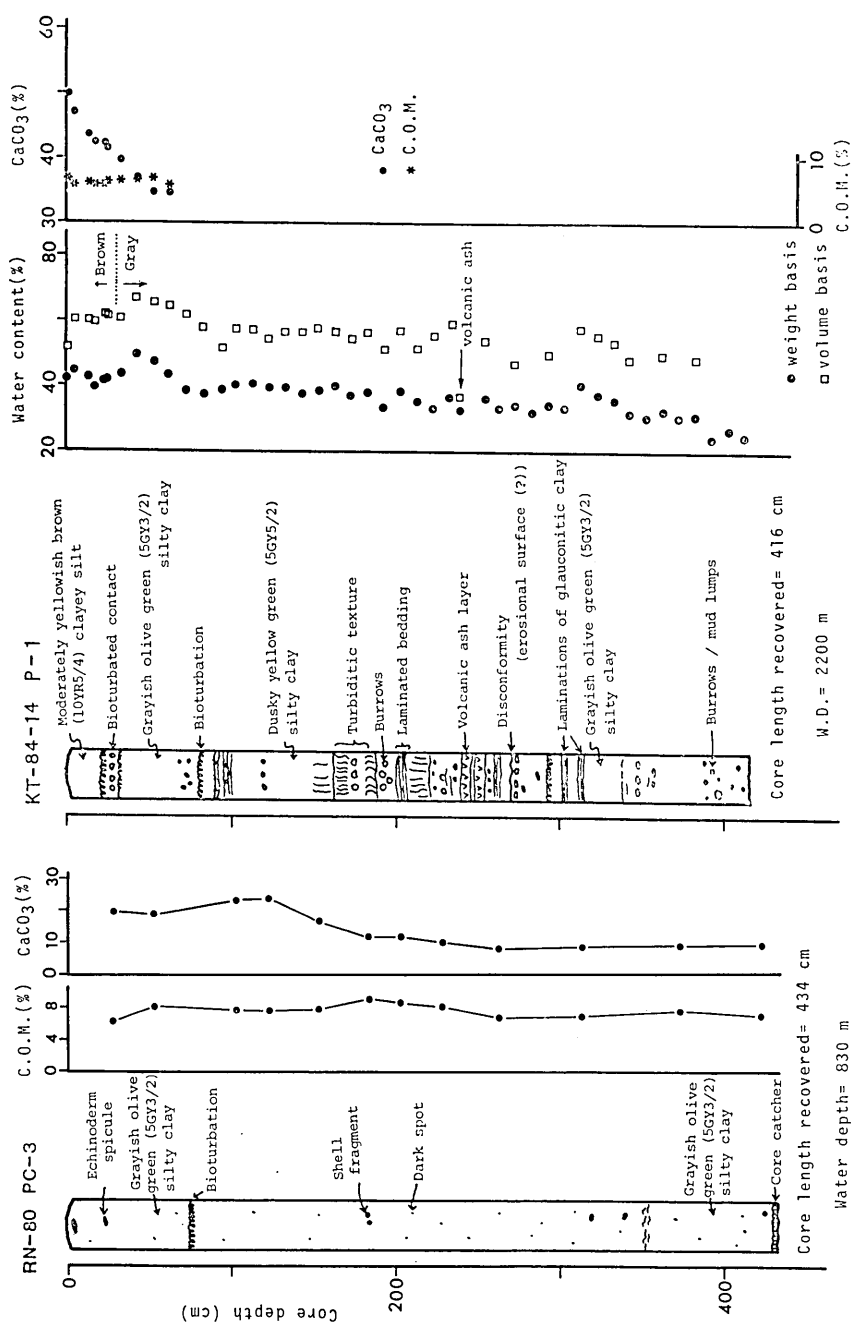


Fig. V-12. Lithologic descriptions of piston cores from continental slope and trench slope. C. O. M.: Combustible organic matter at 550°C. CaCO₃ (%) was estimated from amount of CO₂ (%) by loss on ignition between 550°C and 950°C and by addition of Ca (%) in proportion to CO₂ (%).

The insoluble residue was filtered by a glassfiber filter (GS-25, pore size 1, filtering area 9.6 cm²) and weighed after drying. On the other hand, the filtered solution was brought to exactly 50 ml with distilled water and 13 elements (Ca, Sr, Na, K, Fe, Mg, Mn, Cu, Ni, Zn, Cr, Co, Pb) in the solution were analyzed by atomic absorption spectrometry.

The relation between Ca and the soluble fraction (weight %) by 10% HCl is shown in Fig. V-13A. If Ca is all derived from calcium carbonate (CaCO₃) and the material dissolved by 10% HCl is only CaCO₃, the theoretical relation between them can be represented by the line labeled as CaCO₃ in the figure. The analyzed samples are deviated from this theoretical line, but the observed relation seems to follow a certain line (broken line in Fig. V-13A). The deviation may be related to the fact that the minute particles passed through pores are counted as soluble fraction and also to the fact that the clay minerals contained in the carbonate-rich samples will be leached more easily by HCl than those in the carbonate poor samples. The carbonate contents of the sediments in the Okinawa Trough and its adjacent sea floors (RN-82 D-6) are intermediate between the calcareous sediments off the Okinawa Islands and in the trench slope (KT-84-14 P-1) and the arkosic sands in the continental shelf (Rn-84 SM-1 to 3), according to the clusters observed in Fig. V-13A.

The arkosic sands in the continental shelf, calcareous muds in the trench slope, and brown muds in the Okinawa Trough are clustered also in the K-Na plots shown in Fig. V-13B, except RN81-D-4A of the Okinawa Islands which is non-calcareous sand with quartz and chert fragments. As illustrated in this figure, the Na contents in sediments is related to the seawater contents of sediments. K is contained more in the terrigenous clay because such clay minerals as kaolinite and illite (BERNER, 1971) in the terrigenous clay can absorb K more than pelagic clay. K is more leached from the grayish mud than from the brownish mud. In this respect, the brown mud in the Okinawa Trough is very fine-grained and may be pelagic in origin.

The pelagic origin of the brown mud in the Okinawa Trough is also supported by the Fe-Mg plots in Figs. V-13C and V-13D. The muddy samples including both brown and grayish mud (DE84-D-7a) in the Okinawa Trough are clustered in the Fe-Mg plots; however, the brown muds of the Okinawa Trough are plotted on a straight line almost parallel to the [Fe(%):Mg(%):=3:1] line (Fig. V-13C). Other types of sediments are clustered in other areas and the correlations and the ratio of Fe and Mg in the Okinawa Trough brown mud appear to differ from other samples. If we compare the Fe-Mg relation with the pelagic brown mud in the Ogasawara Trench slope KH-80-1, Sts 4 and 5 (YAMAMOTO and

OOMORI, 1984) on the basis of the concentrations leached by 10% HCl (Fig. V-13D), the composition of the Okinawa Trough brown mud will be understood to be different from the terrigenous sediments and to be similar to the pelagic reddish clay of the Ogasawara Trench slope whose origin may be associated with clay mineralization of deep-sea intermediate to basic igneous rocks (YAMAMOTO and OOMORI, 1984).

In the Fe-Mg plots, the calcareous sediments off the Okinawa Islands are plotted in the high-Mg area and the plots may suggest that the calcareous sediments off the Okinawa Islands are rich in high-Mg calcite as skeletal calcareous organisms. Mn, Zn and other heavy metals are concentrated in some samples. Mn is enriched characteristically in the reddish silty clays in the Okinawa Trough and the surface layer of the KT-84-14 P-1 core. There is a tendency for Zn, Cu, Pb and Co to be slightly enriched in the Okinawa Trough brown mud; particularly, in the DELP-84 D-7b sample. The enrichment in brown mud may be caused by the igneous supply from the axis of the Okinawa Trough.

6. Geology and structure

The surface geology of sedimentary and igneous rocks in the study area is shown in Fig. V-14. The central graben region in the eastern half of the middle Okinawa Trough is composed mostly of igneous rocks and of fairly thick sedimentary layers in the western half. The sedimentary layers are probably Pleistocene and younger in age. In the northern end of the study area, a large volume of rhyolitic pumice blocks and several pieces of basalt were recovered from the small knoll (D-1) (Fig. V-3 and Table V-1) in the Io Deep which is adjacent to the Karuishi Knoll (KK in Fig. V-3) (KIMURA, 1983). From the Karuishi Knoll a large volume of dacitic pumice blocks had been recovered (HONZA, 1976). Judging from diving observations by the submersible "SHINKAI 2000" into area A (UYEDA *et al.*, 1985) and its large volume suggests that the pumice is *in situ*. The K-Ar age of basalt from the central knoll in the Io Deep is 0.29 ± 0.78 Ma (Table V-7), and the fission track age of rhyolite pumice in the same station is 0.07 ± 0.02 Ma (Masao HAYASHI, 1986, personal communication). Pieces of dacitic pumice were obtained from the surrounding knolls. A lot of basalt was obtained from the Iheya Ridge (D-5 and D-6 in Fig. V-3) and dacitic pumice was obtained from the surrounding knolls (D-134 and D-3 in Fig. V-3).

The geologic map in the vicinity of the Iheya Ridge is shown in Fig. V-8, in which the distribution of igneous rocks is presented. Based upon the topographic and geologic information, the Iheya Ridge is considered to have been formed in the latest stage of the igneous activity of the area.

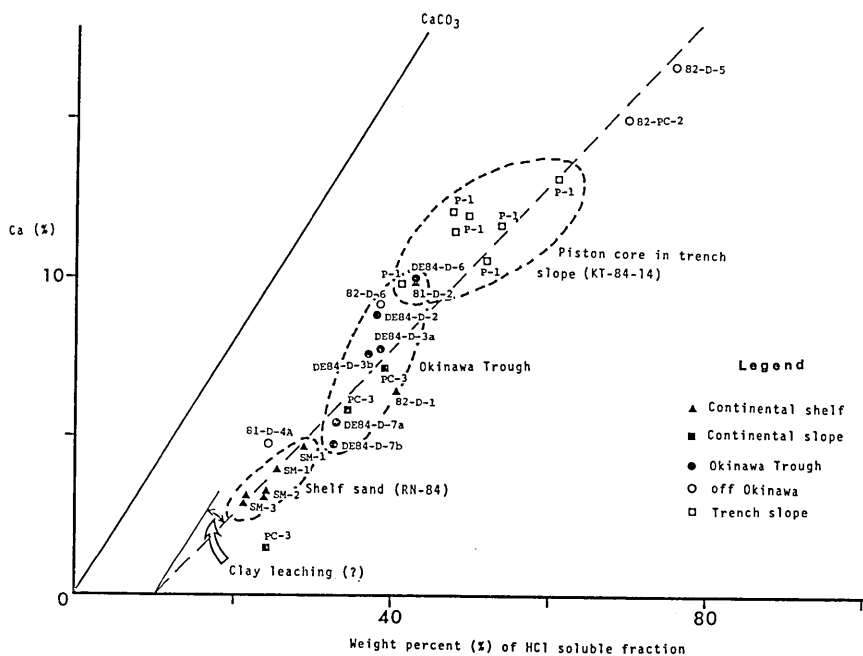


Fig. V-13 (A). Relationship between Ca (%) and weight percent of HCl soluble fraction of sediments. More explanations are given in text.

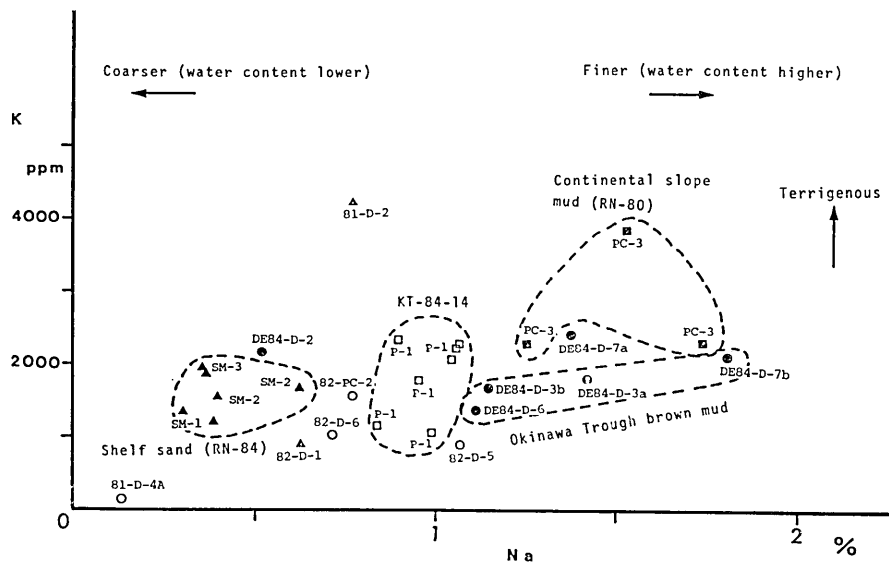


Fig. V-13 (B). Relationship between K (ppm) and Na (%) of sediment.

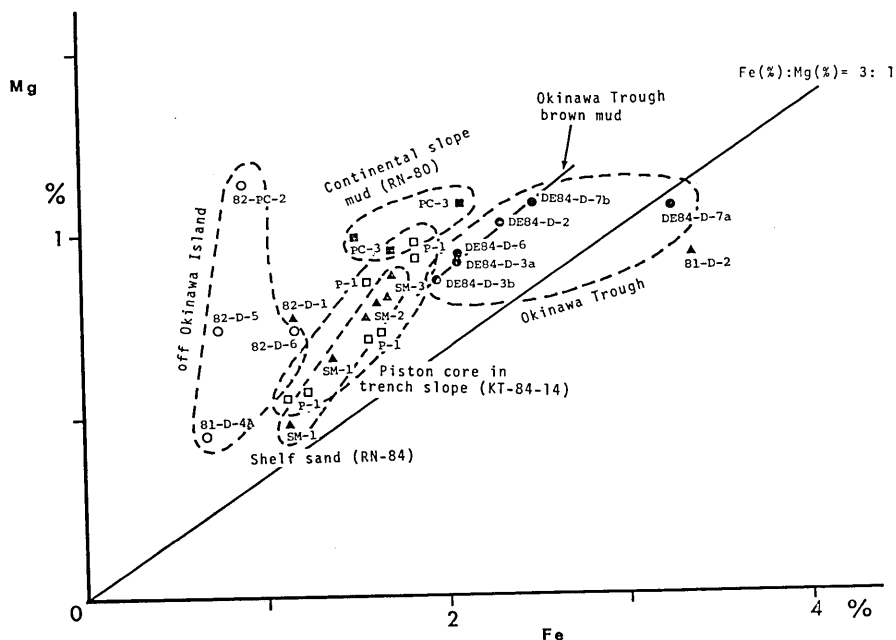


Fig. V-13 (C). Relationship between Fe (%) and Mg (%) of sediments.

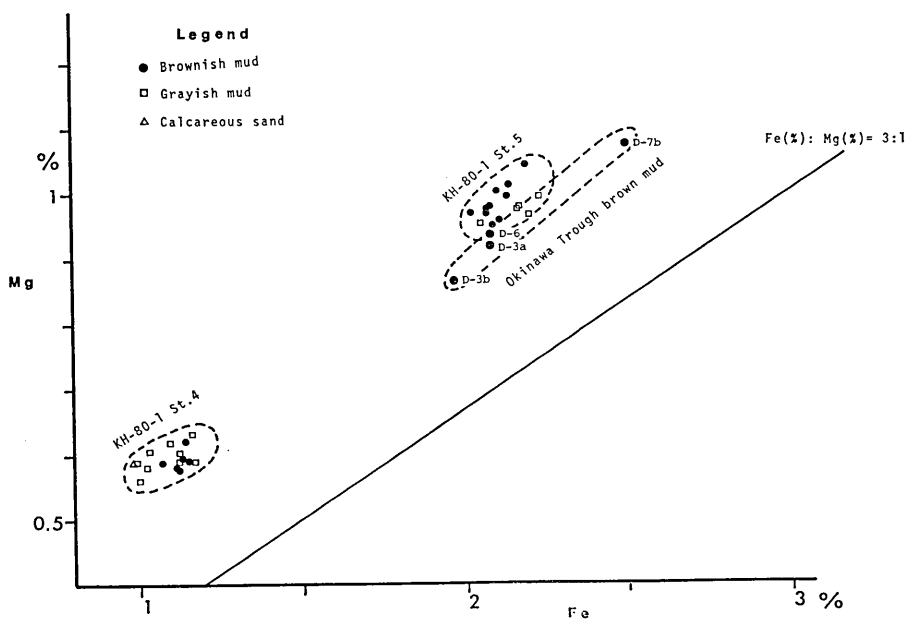


Fig. V-13 (D). Comparison of the Okinawa Trough brown muds and the Ogasawara Trench slope pelagic muds (KH-80-1 St. 4 and 5) in Fe-Mg diagram. Concentrations on both samples are based on leaching by 10% HCl.

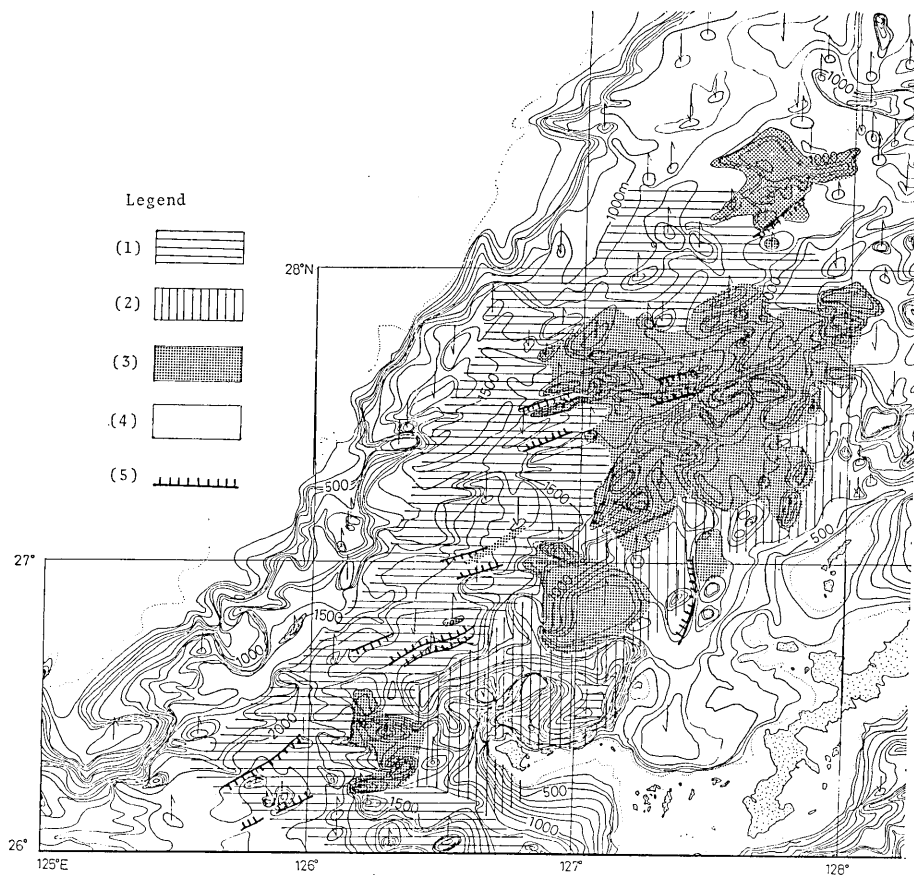


Fig. V-14. Submarine geologic map resulted from the present study. (1) Unconsolidated Quaternary sediments, (2) Semi-consolidated upper Miocene—early Pleistocene sedimentary layer, (3) Igneous bodies, (4) Unidentified area and (5) Active fault, teeth on down-thrown side.

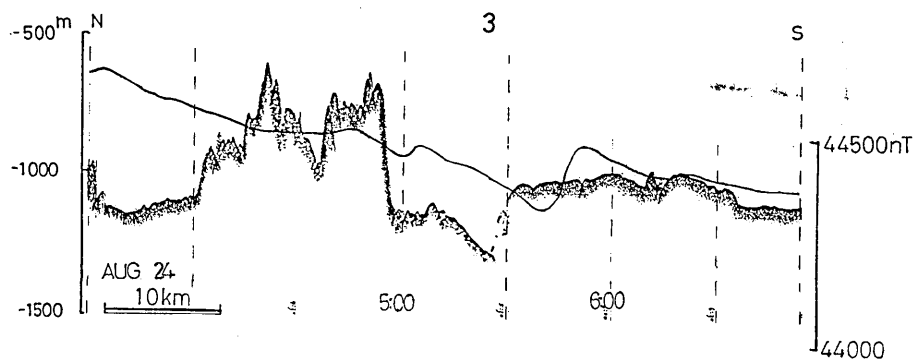


Fig. V-15 (A). Io Deep. Line 3, showing the central knoll between 5:00 and 6:00.

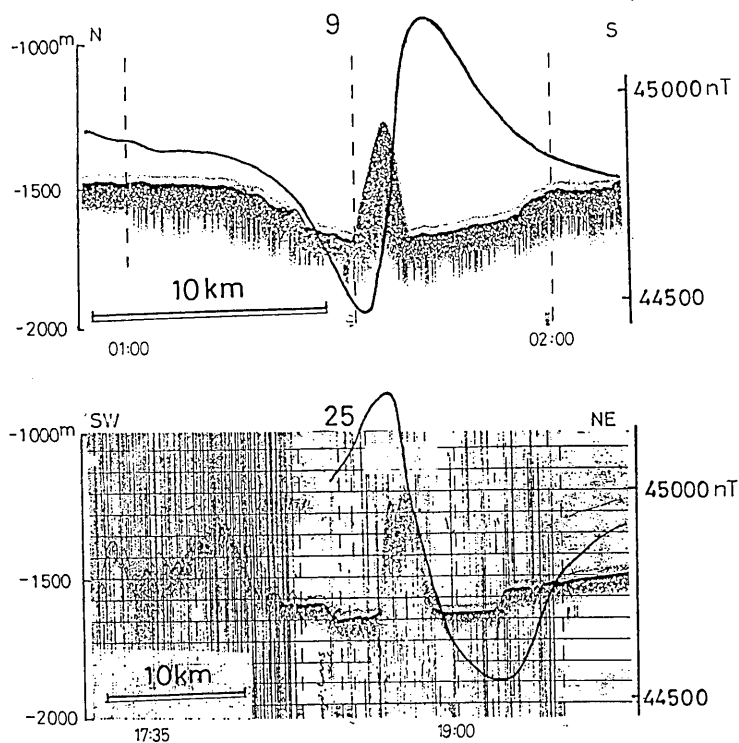


Fig. V-15 (B). Lines 9 and 25 showing the Iheya Ridge.

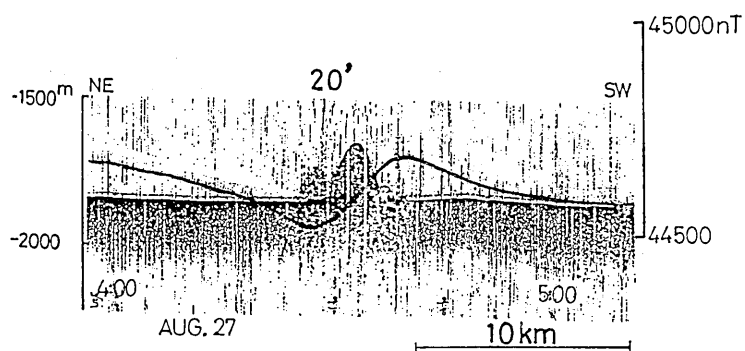


Fig. V-15 (C). Line 20' representing the central knoll in the Aguni Deep.

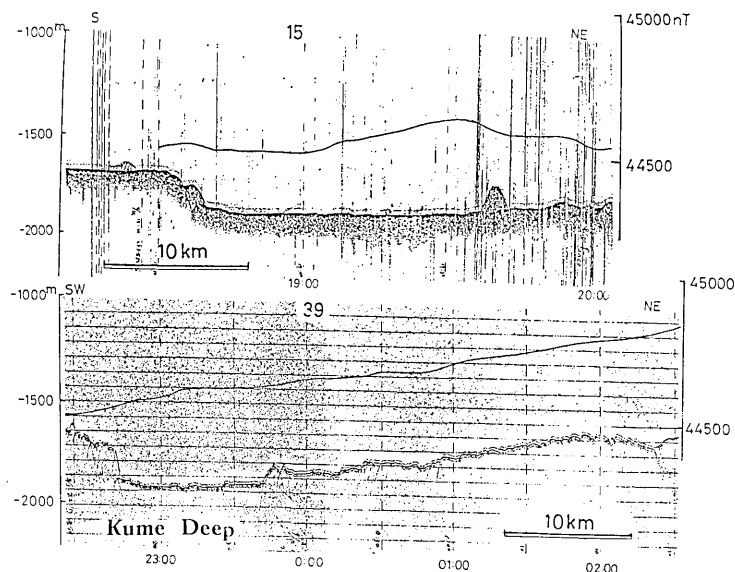


Fig. V-15 (D). Line 15 showing the central knoll in the Kume Deep. Line 39 shows the western part of the Kume Deep where the central knoll and magnetic anomaly are not clear.

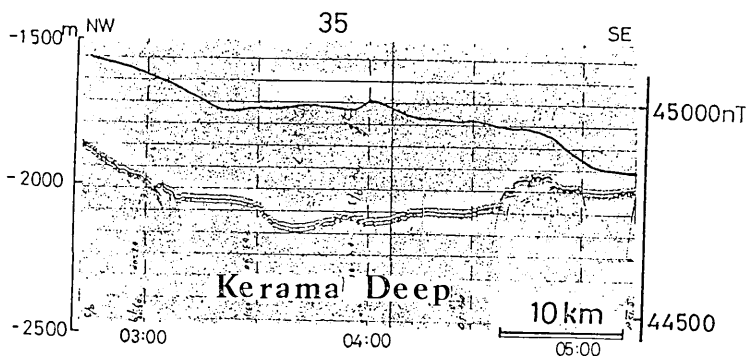


Fig. V-15 (E). Kerama Deep shows a small central topographic high and magnetic anomaly.

Fig. V-15. Examples of topographic and magnetic profiles (total force) across central grabens of the middle Okinawa Trough. Locations are shown in Fig. V-2.

7. Central grabens

The position and structure of the central grabens were determined by seismic reflection profiles, PDR profiles and magnetic profiles (Fig. V-15). Five grabens, i.e. the Io, Iheya, Aguni, Kume and Kerama Grabens were recognized in echelon arrangement along the axis of the middle

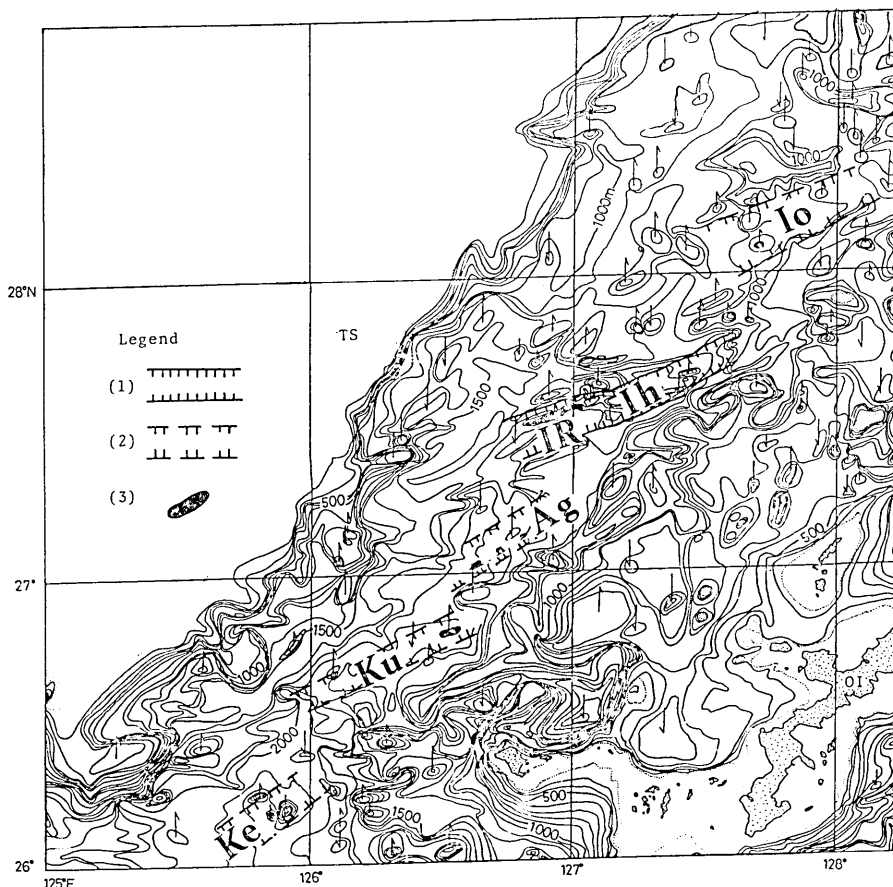


Fig. V-16. Distribution of central grabens and the basaltic central ridge or knolls. Io; Io Graben (central graben), Ih; Iheya Graben, IR; Iheya Ridge, Ag; Aguni Graben, Ku; Kume Graben and Ke; Kerama Graben. Legend: (1) Central Graben rifting igneous bodies; (2) central graben offsetting sedimentary layers; (3) Central ridge or knolls composed of basalt. Basalt samples were dredged by the R/V Jean Charcot in 1984 from the Aguni Graben (SIBUET *et al.*, 1986).

Okinawa Trough in the study area (Fig. V-16). There exists a central ridge in the Iheya Graben and central knolls in the axis of the Aguni, Io, Kume and Kerama Grabens (Figs. V-14 and V-16). Fig. V-15 shows the profiles crossing the central grabens. Figs. V-15B and V-15C show central ridges with marked magnetic anomalies. Figs. V-15A, V-15D and V-15E show central knolls with less marked magnetic anomalies. It is suggested that in these grabens igneous intrusion is at greater depths.

In summary, all of the five central grabens have a central volcanic

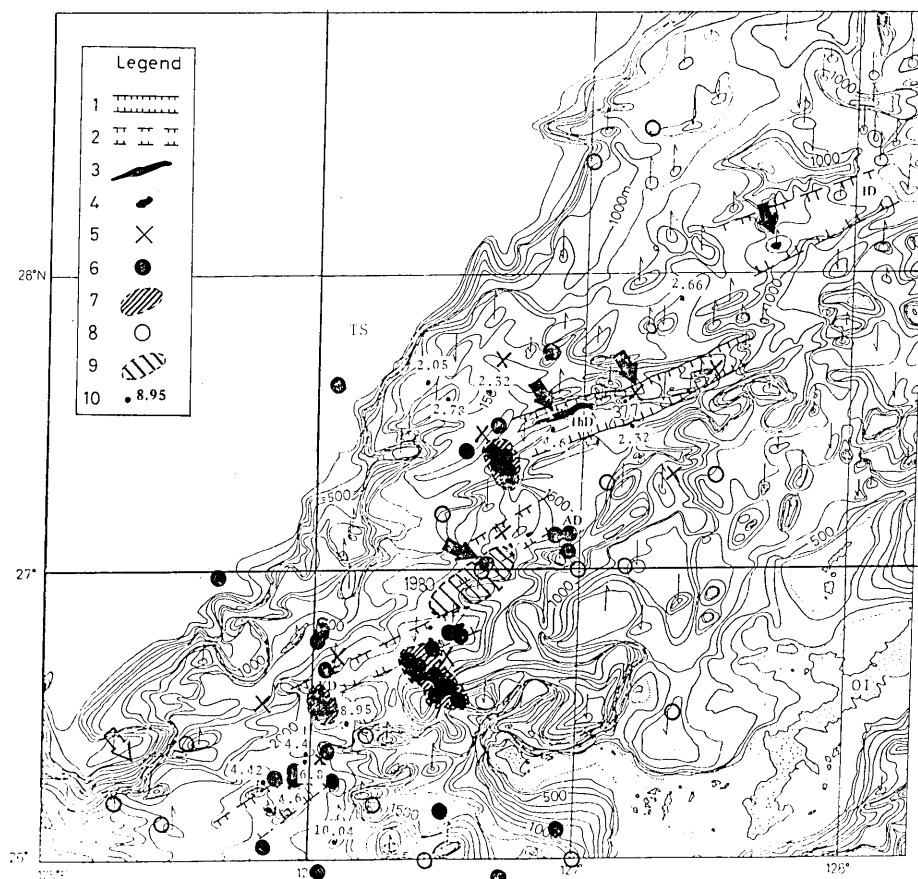


Fig. V-17. Compiled map showing active features of the middle Okinawa Trough. Legend: (1) Central graben in the volcanic area, (2) Central graben in the sediments, (3) Central ridge, (4) Central knoll, (5) Location of OBS by DELP-84 WAKASHIO Cruise, (6) Epicenter determined by the OBS, (7) Earthquake swarm observed by the OBS, (8) Recent epicenter by JMA, (9) Earthquake swarm observed by JMA in 1980, (10) Heat flow value represented in the heat flow unit (HFU) (YAMANO *et al.*, 1986; YASUI *et al.*, 1970), including those of DELP-84 WAKASHIO Cruise and of previous works. Black arrows show location where Quaternary volcanics were recovered by various organizations and the white arrow in the lower left corner represents the location of large shells (HONZA, 1976) which were identified as *Calypptogena* sp. (KOICHI NAKAMURA, 1986, personal communication).

ridge or knolls which may be composed of basalt younger than 0.6 Ma in age. These central knolls and ridges are characterized by normal magnetic anomaly.

The main structural orientation of the central grabens is oblique to the general strike of the arc and characterized by an en echelon pattern

with a left stepping arrangement. Fig. V-17 shows very high activity along the central grabens. Although the bathymetric map suggests some transverse structures between these central grabens, we did not observe any conspicuous faults cutting the NE trending features. The Iheya and Aguni Grabens are roughly parallel and may partly overlap. No transform faults offsetting the grabens were found. This situation is considered to represent the very primitive stage of a spreading system that is not yet well organized. Thus, the middle Okinawa Trough area is concluded to be in a rifting stage of an incipient spreading process.

References

- BERNER, R. A., 1971, Principles of Chemical Sedimentology: McGraw-Hill Book Co., New York, 240 p.
- DALRYMPLE, G. B. and J. G. MOORE, 1968, Argon 40: excess in submarine pillow basalts from Kilauea volcano, Hawaii, *Science*, **161**, 1132-1135.
- DYMOND, J. and L. HOGAN, 1973, Noble gas abundance patterns in deep-sea basalts—primordial gases from the mantle. *Earth Planet. Sci. Lett.*, **20**, 131-139.
- HONZA, E. (Ed.), 1976, Ryukyu Island (Nansei-Shoto) Arc GH 75-1 and GH 75-5 Cruises, January-February and July-August 1975. *Cruise Rep., Geol. Surv. of Japan*, **6**, 81 p.
- KATO, Y., 1986, Woody pumice generated with submarine eruption. *Jour. Geol. Soc. Japan*. (in press).
- KIMURA, M., 1983, Submarine Topography around Ryukyu Arc, Scale 1:1, 180,000. Okinawa Times Press.
- KIMURA, M., 1985, Back-arc rifting in the Okinawa Trough. *Marine and Petroleum Geology*, **2**, 222-240.
- KONDA, T., 1974, Bimodal volcanism in the Northeast Japan Arc, *Jour. Geol. Soc. Japan*, **80**, 81-89 (in Japanese with English abstract).
- KUNO, H., 1954, "Kazan oyobi Kazangan": Iwanami-Shoten, Tokyo, 255 p. (in Japanese).
- LIPMAN, P. W., H. J. PROSTKA and R. L. CHRISTENSEN, 1972, Cenozoic volcanism and plate-tectonic evolution of the Western United States. I. Early and middle Cenozoic. *Phil. Trans. Roy. Soc. London, A*, **271**, 217-248.
- MASUZAWA, T., 1983, Changes of oxidizing-reducing environments in the bottom waters of the Sea of Japan. *Marine Science Monthly*, **15**, 68-77 (in Japanese).
- NIINO, H. and K. O. EMERY, 1969, Sediments of shallow portions of East China Sea and South China Sea. *Geol. Soc. Am. Bull.*, **72**, 731-762.
- SHIBATA, K., S. UTSUMI, K. UTO and T. NAKAGAWA, 1984, K-Ar age results—2—new data from the Geological Survey of Japan. *Bull. Geol. Surv. Japan*, **35**, 331-340.
- SIBUET, J.-C., J. LETOUZEY, F. BARBIER, J. CHARVET, J.-P. FOUCHER, T. W. C. HILDE, M. KIMURA, L.-Y. CHIAO, B. MARSSET, C. MULLER and J.-F. STEPHAN, 1986, Tectonics in the Okinawa Trough: constraints on backarc basin models of formation and evolution, submitted to *J. Geophys. Res.*
- STEIGER, R. H. and E. JÄGER, 1977, Subcommission on geochronology: Convention on the use of decay constants in geo- and cosmo-chronology. *Earth Planet. Sci. Lett.*, **36**, 359-362.
- UJIIÉ, H., S. YAMAMOTO, M. OKITSU and K. NAGANO, 1983, Sedimentological aspects of Nakagusuku Bay, Okinawa, subtropical Japan. *Galaxea*, **2**, 95-117.
- UYEDA, S., M. KIMURA, T. TANAKA, I. KANEOKA, Y., KATO and I. KUSHIRO, 1985, Spreading center of the Okinawa Trough. *Technical Rep. JAMSTEC, Special Issue* **16**, 123-

142 (in Japanese with English abstract).

YAMAMOTO, S. and H. UJIE, 1983, Calcareous sediment around coast of the Okinawa-jima Island. *News Osaka Micropaleontologists*, **11**, 48-62.

YAMAMOTO, S. and T. OOMORI, 1984, Bottom sediment and distribution of metallic elements in 8260m deep ocean floor. *Jour. Geol. Soc. Japan*, **90**, 17-32. (in Japanese with English abstract).

YAMAMOTO, S., S. YADA, M. KIMURA and Y. KATO, 1984, Bottom samples collected from the East China Sea during oceanographic cruises of 1979 through 1983. *Bull. Coll. Sci., Univ. Ryukyus*, **38**, 117-130. (in Japanese with English abstract).

YAMANO, M., S. UYEDA, H. KINOSHITA and T. HILDE 1986, Heat flow measurements in the Middle Okinawa Trough. Part IV, *Bull. Earthq. Res. Inst., Univ. Tokyo*, **61**, 251-267.

DELP 1984 年度中部沖縄トラフ研究航海報告

V. 中央地溝および付近の地形・地質

木村政昭¹, 兼岡一郎², 加藤祐三¹, 山本 聡¹,
久城育夫³, 徳山英一⁴, 木下 肇⁵, 伊勢崎修弘⁶,
正木秀子¹, 押田 淳¹, 上田誠也², T.W.C. HILDE⁷

1) 琉球大学理学部, 2) 東京大学地震研究所, 3) 東京大学理学部, 4) 東京大学海洋研究所, 5) 千葉大学理学部, 6) 神戸大学理学部, 7) Department of Geophysics, Texas A and M University

ドレッジ試料・地震探査反射記録・地磁気探査記録・精密音響測深記録等より、沖縄トラフ中央地溝の地形・地質および地質構造を調べた。その結果、本域の中央地溝は雁行状に配列した5つの切片に分かれることが明らかとなった。そしてその5つの中央地溝のグラーベンの中軸には小海嶺あるいは尖礁状の地形が存在することが発見された。中央地溝の中でも最長のものは、伊平屋海凹と呼ばれるもので、その中軸に見い出される海嶺（伊平屋海凹中央海嶺；仮称）は幅は最大 3 km ほどで長さは 30 km ほどある。ここでは顕著な正の地磁気異常が観測された。今回その海嶺から olivine augite basalt, olivine-bearing augite basalt 等が得られ、化学分析の結果、それらが島弧に特徴的な高アルミナ玄武岩であることがわかった。同岩石の K-Ar 年代は 0.42 ± 0.19 Ma より若いという結果を示し、地磁気異常と調和的である。その周辺からは rhyolite, dacite, acidic, andesite 等が得られた（従来の試料も含む）が、それらは皆第四紀のもので、中央地溝付近では bimodal な噴火活動がおこなわれているとみられる。また、中央地溝中にみられる堆積物は、brown mud が特徴的で、それには Zn, Cu, Pb, Co がやや多い傾向がある。それらは、沖縄トラフ中軸の火山岩からもたらされた可能性が強い。また、雁行状に配列した中央地溝と中央地溝を連結するような、いわゆるトランスフォーム断層に相当するような断層は見い出されなかった。以上の結果は、沖縄トラフ中部域が現在、海底拡大に先行する“大陸地殻のリフティング期”にあることを示しているものと考えられる。